Thiokol
REACTION MOTORS DIVISION

GAS MIXTURES FOR DYNAMIC SIMULATION OF ROCKET EXHAUST JETS

Report: RMD 5804-F
Contract: NAS 8-20057
Period: 4/12/65 - 11/11/65
Date: 11/23/65

Prepared for George C. Marshall Space Flight Center
Huntsville, Alabama

Walter R. Marsh

Approved by: Albert D. Corbett
Albert D. Corbett
Section Supervisor
Research Engineering Dept.

Steven J. Tunkel
Steven J. Tunkel
Manager
Research Engineering Dept.

David J. Mann
David J. Mann
Director of Research

FOREWORD

This is the final progress report describing work performed by Thiokol Chemical Corporation, Reaction Motors Division, Denville, New Jersey under NASA Contract NAS-8-20057. The work was performed under the cognizance of Messrs. Benford Johnson and Dale Andrews, NASA Marshall Space Flight Center, Huntsville, Ala.

The research effort reported herein was conducted during the period 12 April 1965 to 11 November 1965 on RMD Project 5804. The report was prepared by Mr. W. Marsh who was also technical program manager. The work was performed under the cognizance of Mr. S. Tunkel, Research Engineering Dept. Manager and Mr. A. Corbett, Section Supervisor. Principal contributors in addition to the above, were Messrs. E. Davis and G. Brown of the Scientific Analysis Section and G. Itani of the Research Engineering Dept. Additonal contributions to the effort were made by personnel of the Test Dept. as required.

ABSTRACT

A program of analytical and experimental research leading to selection of a gas mixture for dynamic simulation of rocket exhausts has been conducted at Thiokol Chemical Corporation, Reaction Motors Division. Analytical work involved screening and evaluation of many candidate gaseous compounds for their applicability to gamma, Mach number and viscous flow similitude.

Nozzle flow tests were conducted with nitrogen, CF_4, $CHClF_2$, and mixtures of the same. Results were used in determining the validity of theoretical computations performed on mixtures. Mixtures of CF_4 and N_2, with C_2F_6 as an optional additive were selected as being capable of simulating a range of rocket engine system parameters. $C_2H_2F_2$ was selected as an alternate additive to replace C_2F_6. The relative advantages of these simulants over hot flow H_2O_2 decomposition products, SF_6 or neat nitrogen are shown.

Author

TABLE OF CONTENTS

TABLE OF CONTENTS (Con't)

LIST OF ILLUSTRATIONS

NOMENCLATURE

A	Area, $ft.^2$
a,b	VanderWaal's constants
c*	characteristic velocity, fps
C_p	specific heat at constant pressure
C_v	specific heat at constant volume
d	diameter of flow passage, ft.
D	equivalent diameter of heater, ft.
g	weight of a constituent, lb.
G	mass velocity per unit cross sect. $lb/sec-ft.^2$
H	heat transfer coefficient, $BTU/sec-ft^2-^oF$
Isp	specific impulse, lbf.-sec./lbm.
K	Thermal conductivity, $BTU/sec-ft.-^oF$
L	length used in Reynolds number, ft.
M	Mach number
M_i	molecular weight of i th constituent
$\bar{M}$	mean molecular weight
n	number of moles
P	pressure, psia
Q	Heat flux, BTU/sec
R	ideal gas constant
R_e	Reynolds number
T	temperature (specified units)

t	time, sec.
V	volume, $ft.^3$
v	velocity, ft/sec
$\dot{w}$	weight flow rate, lb/sec
w	weight, lb.
x	distance along nozzle axis, in.
ϵ	nozzle area ratio (Ae/At)
γ	ratio of specific heats at a point
$\bar{\gamma}$	effective ratio of specific heats through process
μ	viscosity, (micropoise, unless specified)
ρ	density, lb/ft^3, sl/ft^3, or g/cc
δ	boundary layer thickness
θ_n	nozzle exit half angle

SUBSCRIPTS

A	actual
a	average, or ambient
c, ch	chamber
e, ex, exh	exhaust (exit plane)
L	based on L
M	model
n	nth node
o	first, or initial
r	regulator outlet

t	throat
tk	tank
v	valve

I. INTRODUCTION

A. General

The simulation of exhaust jets in model experiments in wind tunnels previously has assumed calorifically ideal gases in both the model and full-scale missile engines. This assumption implies that the ratio of specific heats, $\gamma = c_p/c_v$, is a constant. In rocket engine expansions the specific heat ratio is not constant. Due to the changing chemical composition throughout the expansion cycle, the assumption of constant molecular weight is also in error. Furthermore, gases having a gamma significantly different than the actual engine have been used in previous simulation work.

The purpose of this program is to select simulant gas mixtures applicable to small scale simulation of large clustered rocket engines. Both analytical and experimental research leading to selection of such a simulant has been conducted to screen candidate gases for their ability to simulate the rocket engine combustion gases. The simulant flow parameters have been investigated for their ability to match three principal similarity laws involving specific heat ratio (γ), Mach number and the viscous flow parameter $\rho v/\mu$. These similarity laws are expressed below.

$$(P_a / P_e)_M = (P_a / P_e)_A \qquad \text{Pressure Ratio}$$

$$\left(\frac{\gamma_e M_e^2}{\sqrt{M_e^2 - 1}}\right)_M = \left(\frac{\gamma_e M_e^2}{\sqrt{M_e^2 - 1}}\right)_A \qquad \text{Turning Angle}$$

$$\frac{d_A}{d_M}\sqrt{\frac{x_M}{x_A}\left(\frac{\mu_M}{\mu_A}\right)\left(\frac{\rho_A}{\rho_M}\right)\left(\frac{v_A}{v_M}\right)} = 1 \qquad \text{Viscous Flow}$$

The first two similarity rules have been met by simultaneous matching of gamma and Mach number, since it is believed that errors occur when using the turning angle similitude rule. The required values of gamma have been obtained by preparation of gas mixtures having both low and high gamma components. Proper Mach numbers were obtained by adjustments in the expansion ratio. Viscous flow similitude is met by simultaneous tailoring of the velocity, density and viscosity of the gas mixture, by temperature control,

and by adjusting the length and scaling factor of the nozzle. Analysis of the jet outside of the nozzle was performed on one of the simulants to determine the Mach number, gamma, and viscous flow variations there.

This final report describes the work accomplished during the period from April 12, 1965 through November 11, 1965.

B. Summary of Previous Research

In recent efforts to simulate the clustered engines of the Saturn V booster in small scale tests in wind tunnels, the properties of the exhaust jet and the base pressure and circulation were not in agreement with the full scale tests when both were made at sea-level conditions. At altitude conditions, the wind-tunnel tests did not agree with theoretical results, and it is believed that the actual engines may also produce different results at altitude.

There are many plausible analytical reasons why model tests and full scale tests will disagree even when similitude is maintained according to the pressure ratio and turning angle rules. According to Hensel (Ref. 10), the assumption of linear theory in turning angle leads to significant error when the ratio of exit to ambient pressure is greater than three. (It was also previously stated that the Prandtl-Meyer turning angle equations would be used if necessary in similitude analyses). Ignoring RT products in a desire to use cold gas simulation, may be another source of error, but there is some experimental evidence that $(RT)_{exh.}$ does not effect the position of the exit and transmitted shock waves. Nevertheless, cognizance of temperature is obtained when scaling viscous effects. It is certain, however, that model experiments must match γ and Mach number simultaneously.

The desire for cold gas simulation has led to the use of air, helium, CO_2, Argon, H_2-CO_2 mixtures, nitrogen, SF_6 and H_2O_2 decomposition products. For rocket engine exhaust gas simulation, all but SF_6 and $H2O_2$ products can be ruled out due to a mismatch in γ or Mach number.

Attempts to achieve a useful simulation with nitrogen or air were apparently unsuccessful due to the large discrepancies in Mach number, gamma, and the density-viscosity combination governing viscous flow scaling. Even though the similarity rules for pressure ratios and turning angles were followed, the excessively high gamma of nitrogen along with the low Mach number which was used to compensate for gamma in the similitude rule were apparently responsible for an erroneous plume shape and intersection pattern. The thick

boundary layer which would build up in the small scale engine with low density nitrogen (or air) was probably responsible for additional obscuring of the plume shape.

Decomposition of 90% H_2O_2 with a gamma value on the upper end of the range for rocket engine simulation has been attempted, but at the high area ratios of interest, some H_2O condenses out of the system rendering the test invalid. This has been true even with 100% H_2O_2 and simulation chamber pressures in excess of 1000 psia.

Sulfur hexafluoride, also used previously, would appear to be an ideal simulant. Although pure sulfur hexafluoride is inert, non-toxic, has a low gamma, and is gaseous down to low temperatures, the commercially available compound contains lower fluorides of sulfur which are highly toxic, and which readily hydrolyze in water to release HF, another highly toxic and corrosive compound.

C. Program Objectives

The objectives of the program as outlined in the Work Statement were as follows:

(1) Gases and mixtures of gases will be screened for their ability to meet the requirements of the various similarity rules shown in the above section. Parameters such as specific heat ratio, viscosity, expansion ratio vs. pressure drop, and the degree of non-ideality will be studied. A method of determining the properties of mixtures other than those specifically tabulated will be provided.

(2) The jet geometry and boundary layer similitude will be studied in accordance with the similarity rules shown above. The ability of the simulants to duplicate the plume intersection geometry will be studied. A computer program will be used to correlate theoretical data with experimental data to evaluate the effects of various simulants and nozzle geometrics on the boundary layer and plume geometry.

(3) Experiments will be conducted using the selected candidate simulant gases to experimentally determine the effective specific heat ratio through measurements of the pressure drop through a supersonic deLaval nozzle, and any corrections that may be required in the analytical data will be determined. The exact geometry of the nozzle will be determined by doing a similarity analysis of flow considering boundary layer as outlined above. The nozzle will be tested and redesigned to meet the nozzle similarity requirements under experimental conditions.

(4) Results of the analytical and test programs will be used as a basis for defining a simulant mixture which can be easily modified to encompass a range of similarity parameters. A generalized method for selecting or modifying a mixture is to be developed and provided as a tool with which more specific work can be done. Alternate simulants will also be recommended, and a complete list of all simulants considered will be provided with the results of analytical and experimental studies.

II. SIMULANT GAS SELECTION AND ANALYSIS

A. Criteria for Selection

Simulant selection criteria, based on three similitude rules and other requirements, have been established and the ability of simulants to meet these criteria over a useful range of parameters has been investigated. The selection of simulant candidates was carried out with the requirements of low gamma, high density, low boiling point, low toxicity, low viscosity, and low cost in mind. If any of these conditions were grossly violated, the gas in question was not considered.

The ability of simulants to duplicate the shape of a plume having a changing gamma has been investigated as part of the study. This has been a preliminary investigation pending a specific application.

At the suggestion of NASA, the F-1 rocket engine, using Lox/RP-1 propellants, was taken for some of the sample calculations as a point where comparisons would be made between simulants. Much of the screening of simulants was done using the standard 1000 to 14.696 psia expansion. The following guidelines were set up for the selection of simulant candidates to be more intensively evaluated later.

1. Gamma Requirements. The range of gamma encountered in rocket combustion gases was found to be from 1.06 to about 1.35. Most of the values range from 1.15 to 1.25. Simulant candidates should have as low a gamma as possible. In order to simulate intermediate values of gamma, diluents having higher gammas have been considered for use in mixtures.

   The simulant with the lowest values of gamma was found to be C_2F_6. Nitrogen was found to be a very suitable diluent.

2. Density Requirements. A high density is desirable to meet the viscous flow requirement. It was found that, all other things being equal, the highest available density would be most desirable. In general, an average density of more than 0.15 lb/ft^3 at S.T.P. is mandatory for a mixture. C_2F_6 and $CBrF_3$ were found to be good from this standpoint.

3. Boiling Point. The boiling point at one atmosphere pressure gives an approximate indication of the relative vapor pressures over the entire temperature range of interest. For the purpose of preliminary screening, only gases with boiling points less than -100°F were considered. It has since been found that, to avoid condensation in the plume near a wind tunnel model, a boiling point of -100°F or less depending on Mach number and altitude may be required. Therefore, final consideration was given only to those simulants having boiling points less than -100°F. CF_4 was found to be the lowest-boiling low-gamma simulant. A vapor pressure diagram for several candidate simulants appears in Figure 1.

4. Toxicity. After a wind tunnel run, the tunnel atmosphere will be contaminated with small amounts of simulant. The simulants should not be toxic to personnel working on the model after a run. There should be no toxic decomposition products nor flammable mixtures which also rules out thermally unstable or combustible gases. Temperatures of 700 to 1000°F were assumed to be reached during tunnel operation.

5. Cost Limitations. Cost was considered after the preliminary screening eliminated most of the combustible, unstable, toxic and higher-boiling compounds. A cost of $5.00/lb was considered the practical limit for any component of a mixture and an average cost of less than $3.00/lb was considered desirable. Most simulants which meet the other requirements are marginal from this viewpoint.

6. Viscosity Requirements. The viscosity affects the viscous flow parameter and should be as small as possible. A value of less than 100 micropoise at the exit plane would be desirable but is obtained only with some of the noble gases which have much too high a gamma. The parameter $(\rho v/\mu)$ was calculated for all of the final candidates and used in the selection and nozzle scaling process.

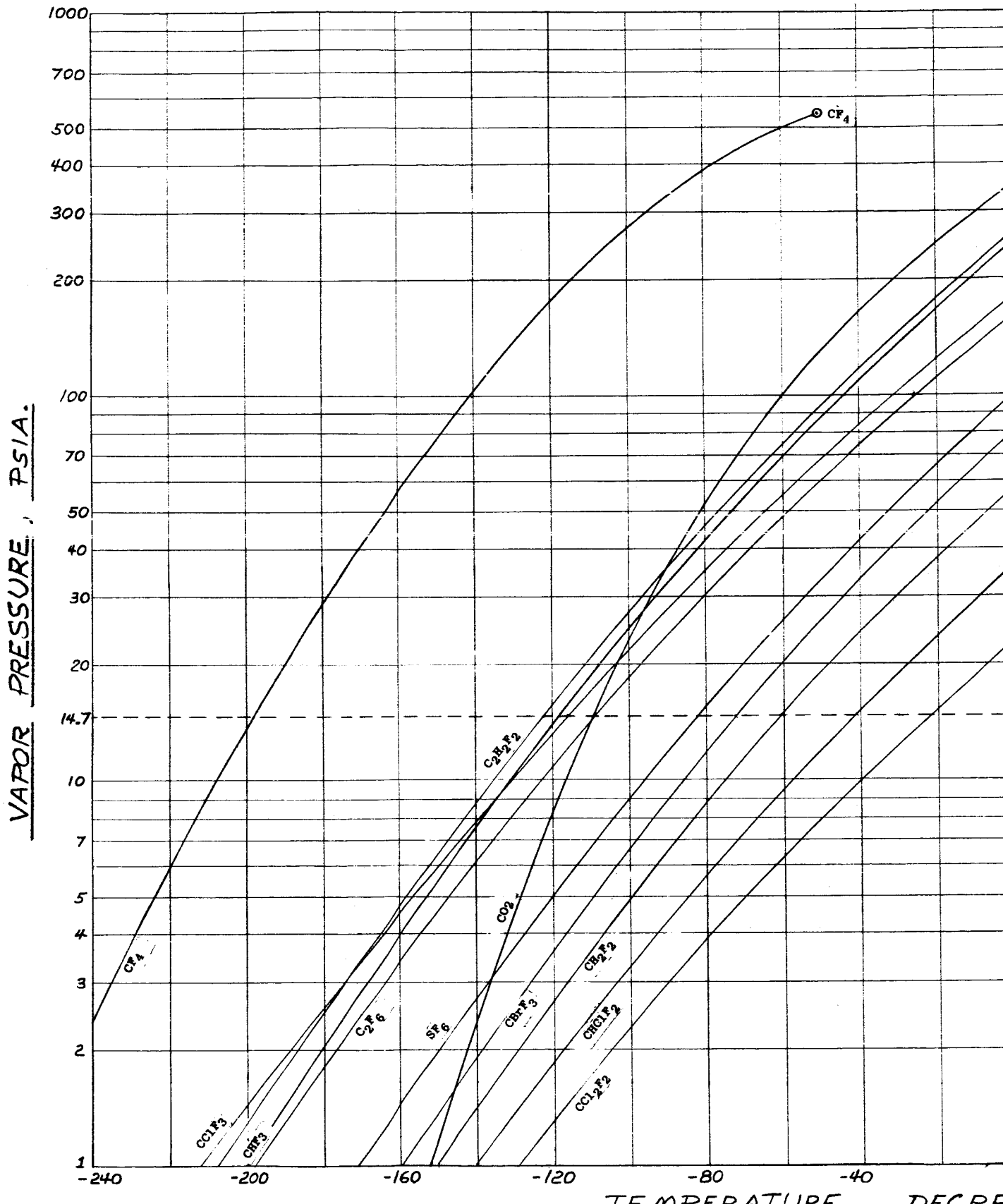

Fig 1

FIGURE 1 VAPOR PRESSURE C

Thiokol

5804-F

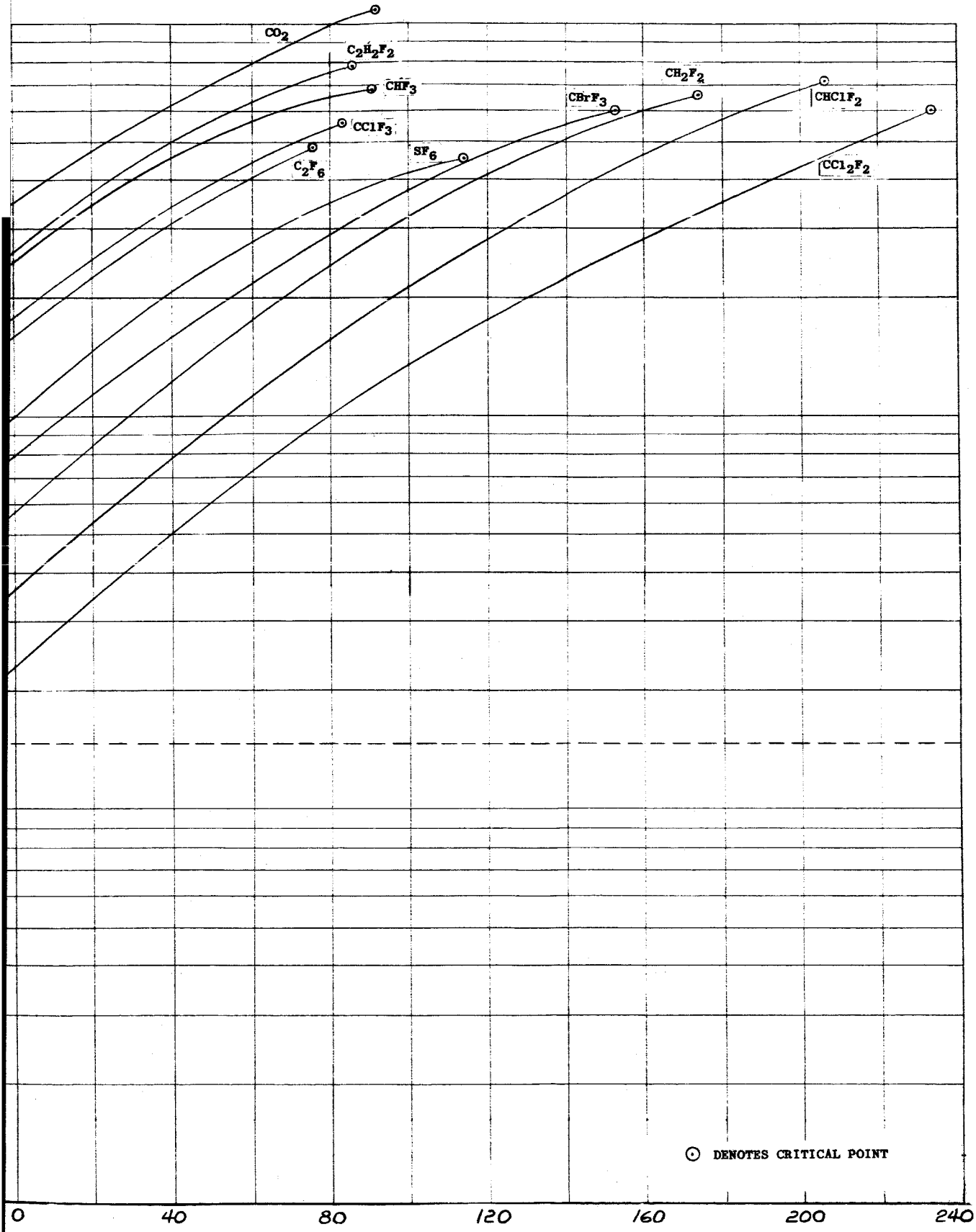

ES FAHRENHEIT

IRVES OF SIMULANTS

Fig 3.1 (2)

The above considerations, if all strictly adhered to for high altitude, high flight Mach number, large engine simulation, would eliminate all known gases in existence. Some have marginal boiling points, some have unacceptable viscous flow parameters, some have too high a gamma, and some are toxic, flammable, or expensive.

For most altitudes and flight Mach numbers of interest, however, gas mixtures have been found which give far better simulation than the previously used methods. These methods, which involve a variety of working fluids, are outlined with their shortcomings in Table I. The approaches which have been taken to alleviate these shortcomings are outlined in Table II.

The requirement of a low gamma points to the need for a polyatomic gaseous molecule. The requirement of a high density leans in favor of heavy molecules, such as those containing chlorine or bromine. A low boiling point leans in favor of molecules having mostly light and/or gaseous elements such as hydrogen and fluorine.

A large number of gases are available, including the hydrocarbon family (such as CH_4, C_2H_4, etc.), the fluorocarbons (such as CF_4) and other miscellaneous gases such as NH_3, SiF_4, SiH_4, CO_2, N_2O, etc. Toxicity (and also flammability, reactivity, and poor thermal stability) rule out the hydrocarbons, silane, and ammonia. The series of hydrocarbons and their fluorine and chlorine-containing counterparts encompass a large number of possible gases. Not all have been synthesized, however, and most are liquid in the temperature range of interest. Figure 2 illustrates the arrangement of possible compounds. The compounds marked with an asterisk have boiling points applicable to the needs of simulation and are non-toxic and non-reactive.

Estimates indicate that gamma does not change very rapidly in the immediate plume (within two exit diameters) either in the actual engine or in the model. Differences in the rates of change in gamma are therefore unimportant, except in the boundary layer which consists of turbine exhaust gases. These gases are expected to have an intermediate gamma between the core and air, due to their low temperature and fuel-rich nature. The effect of the turbine exhaust gas burning in the air is expected to produce some fluctuations of the gamma in the boundary layer, but a complete description of this process was beyond the scope of the program.

TABLE I

VARIOUS METHODS OF SIMULATION
PREVIOUSLY IN USE

Method and Working Fluid	Disadvantages
Cold flow using air or nitrogen	Gamma too high and changes too little. Viscous flow problems.
Hot flow with H_2O_2 decomposition products	Condensation occurs in nozzle. Severe Reynold's No. problem. Gamma still not controllable.
Hot flow with combustion of actual propellants being simulated	Severe Reynold's No. problem. Severe heat and contamination problems.
Cold flow with sulfur hexafluoride	Gamma too low (unless mixed with nitrogen). Highly toxic and corrosive impurities and decomposition products. Marginal boiling point. Viscous flow problem.

TABLE II

APPROACHES TAKEN TO ALLEVIATE
SHORTCOMINGS OF PREVIOUS METHODS

Problem Areas	Approaches to Solution
Gamma too high or too low.	Use of binary or ternary mixtures containing low and high gamma components.
Toxic and corrosive gases and products.	Use of stable, non-toxic inert fluorocarbons and nitrogen.
Viscous flow (Reynold's No.) problems.	Gas mixture optimization. Special nozzle and turbine exhaust inlet configurations.
Boiling point too high, causing condensation.	Use of the lowest-boiling gases available.

METHANE GROUP

CH_4				
CH_3F*	CH_3Cl			
CH_2F_2*	CH_2ClF	CH_2Cl_2		
CHF_3*	$CHClF_2$*	$CHCl_2F$	$CHCl_3$	
CF_4*	$CClF_3$*	CCl_2F_2	CCl_3F	CCl_4

ETHYLENE GROUP

C_2H_4				
C_2H_3F	C_2H_3Cl			
$C_2H_2F_2$*	C_2H_2ClF	$C_2H_2Cl_2$		
C_2HF_3*	C_2HClF_2	C_2HCl_2F	C_2HCl_3	
C_2F_4*	C_2ClF_3*	$C_2Cl_2F_2$	C_2Cl_3F	C_2Cl_4

ETHANE GROUP

C_2H_6						
C_2H_5F	C_2H_5Cl					
$C_2H_4F_2$*	C_2H_4ClF	$C_2H_4Cl_2$				
$C_2H_3F_3$*	$C_2H_3ClF_2$	$C_2H_3Cl_2F$	$C_2H_3Cl_3$			
$C_2H_2F_4$*	$C_2H_2ClF_3$	$C_2H_2Cl_2F_2$	$C_2H_2Cl_3F$	$C_2H_2Cl_4$		
C_2HF_5*	C_2HClF_4	$C_2HCl_2F_3$	$C_2HCl_3F_2$	C_2HCl_4F	C_2HCl_5	
C_2F_6*	C_2ClF_5*	$C_2Cl_2F_4$	$C_2Cl_3F_3$	$C_2Cl_4F_2$	C_2Cl_5F	C_2Cl_6

Figure 2. Possible Compounds in the Hydro-Fluoro-Chlorocarbon Series

B. Analytical Selection Procedure

Once the characteristics of the full scale engine have been obtained, the simulant selection process is undertaken in three steps.

(1) From a list of all available gases, eliminate those which are grossly unacceptable from the standpoints of:

(a) Boiling Point

(b) Toxicity and Reactivity

(c) Cost and Availability

(d) Gamma

(e) ρ/μ (density/viscosity)

The remaining candidates will usually consist of a few fluorocarbons and nitrogen diluent. In general, for smaller full scale engines, the density and viscosity requirements become less stringent as the model scale factor increases. Table III gives a comprehensive list of low boiling gases.

(2) The performance of the remaining candidates is evaluated over a range of temperatures and pressure ratios, using the simulant characterization program discussed in more detail in Appendix A. This program computes gamma, Mach number, density, exhaust temperature, velocity, specific heat, area ratio and other parameters as a function of pressure ratio, chamber temperature, and the gas thermodynamic data. Viscosity may be calculated or estimated from viscosity vs. temperature data or from empirical relationships. Computer programs are usually available to do this.

With this data available, plots of γ_e, M_e, and the viscous flow parameter $\rho v/\mu$ are prepared for the gases over the ranges of temperature and pressure ratio of interest. From these plots, approximate binary and ternary mixtures can be chosen for various pressure ratios which match γ_e and M_e of the actual engine. These mixtures will consist of one gas having a lower gamma than the actual engine and another gas having a higher gamma. From a viscosity standpoint, a low exhaust temperature is desirable, as long as P_e does not exceed the vapor pressure at T_e.

TABLE III. SUMMARY OF SIMULANT CANDIDATE PROPERTIES

NOTES

a. Exit plane gamma; P_c = 1000 psia, T_c = 400°F, and P_e = 14.696 psia.

b. Density of gas at one atmosphere pressure and 70°F.

c. Viscosity in micropoise at exit plane; P_c = 1000 psia, T_c = 400°F and P_e = 14.696 psia.

d. At exit plane; P_c = 1000 psia, T_c = 400°F, and P_e = 14.696 psia.

e. Estimated.

f. Velocity at exit plane in feet/second; P_c= 1000 psia, T_c = 400°F and P_e = 14.696 psia.

g. "Freon 502": DuPont's designation for an azeotropic mixture of 48.8 wt. % $CHClF_2$ and 51.2 wt. % C_2ClF_5.

h. Carrene-7: An azeotropic mixture of $C_2H_4F_2$ and CCl_2F_2.

TABLE III . SUMMARY OF SIMU

Chemical Formula	Boiling Point °F	Critical Temp. °F	Critical Press. psia	Cost $/lb	Typical Gamma(a)	Density (b)
He	-453.8	-450.2	33.2	9.41	1.660e	.0103
N_2	-320.4	-232.8	492.3	0.07	1.394	.0725
Ar	-302.3	-187.6	705.4	1.29	1.668e	.1035
CF_4	-198.4	- 49.9	542.9	5.00	1.156	.227
SiH_4	-169.2	+ 25.7	705.4	400.00		.0827
N_2O	-129.1	+ 97.7	1053.7	0.60	1.298	.1147
$C_2H_2F_2$	-122.3	+ 86.2		1.80	1.138	.167
CHF_3	-115.9	+ 79.	690.9	5.00	1.201	.182
$CClF_3$	-114.6	+ 83.8	561.	4.50	1.138	.286
CH_3F	-109.4	112.8	911.	300.00		.0885
CO_2	-109.3	88.0	1072.8	0.15	1.331	.1146
C_2F_4	-109.0	92.	580.	2.50		
C_2F_6	-108.8	75.8	480.	2.50	1.076	.361
C_2H_3F	- 97.5			3.65		.119
SiF_4	- 85.0	29.3	735.0	1.25	1.150e	.270
SF_6	- 82.0	114.	545.	2.75	1.082	.383
$CBrF_3$	- 72.0	153.		3.00	1.333e	.614
CH_2F_2	- 60.9	173.		10.00	1.260	.150e
$C_2H_3F_3$	- 52.2					
F-502(g)	- 50.1	193.6		1.26	1.147	.173e
$CHClF_2$	- 41.4	205.	716.	0.57	1.177	.227
C_2ClF_5	- 37.7	175.9	453.	2.00	1.117e	.119
C_2H_5F	- 35.9					
C_2ClF_3	- 30.e			2.00		.303
C-7(h)	- 28.0	221.	631.			
CCl_2F_2	- 21.6	234.	597.	0.29	1.125	.333
$C_2H_4F_2$	- 12.5	200.	460.	0.56		.185
CH_3Cl	- 11.6	289.5	969.	0.50	1.282	.1316

Thiokol

5804-F

ANT CANDIDATE PROPERTIES

Viscosity (c)	Mach No. (d)	Toxicity	Reactivity	Exhaust Velocity(f)	Useful As Simulant
		n	n		diluent
108	3.41	n	n	2744.1	diluent
88		n	n	2088.5	diluent
189	3.03	n	n	1819.4	yes
		med.	high		no
117	3.13	low	n	2385.1	?
112	3.04	low	low	2141.9	yes
145	3.04	n	n	2004.2	yes
165	3.03	n	n	1679.4	yes
127e			med.		no
126	3.12	low	n	2374.7	?
		n	n		?
162	2.99	n	n	1518.1	yes
					?
161e					?
193		med.	n	1458.7	no
113	3.06	n	n	1285.4	?
110	3.04			2276.1	no
					?
	3.03	n	n	1624.2	?
135	3.04	n	n	1815.4	no
	3.02	n	n		no
					no
		n	n		no
		n	n		no
140	3.03	n	n	1568.2	no
		low	med.		no
108		med.	high		no

TAB III (2)

The properties of CF_4, C_2F_6, $C_2H_2F_2$, $CClF_3$, CHF_3, $CHClF_2$, $CBrF_3$ and some mixtures have been investigated over a wide range of pressure ratios and temperatures. The tables in Appendix B exemplify the fact that Mach number is primarily a function of pressure ratio only and that γ_e is a function of both temperature and pressure ratio.

Theoretical analyses of the simulants indicate that Mach number and γ_e are linear functions of log (P_c/P_e). Figures 3 and 4 show γ_e and M_e as a function of pressure ratio and chamber temperature for CF_4, C_2F_6 and nitrogen.

(3) After approximate mixtures have been selected from the gamma - Mach number plots for single compounds, these mixtures are evaluated, using the Simulant Characterization Program to determine, by trial and error or by plotting, the correct mixture ratios which provide exact matching of gamma and Mach number simultaneously.

After a group of mixtures (at different pressure ratios and chamber temperatures) are characterized it is necessary to determine if the pressure exceeds the vapor pressure of any of the components during the expansion. Those mixtures having condensation problems must either be eliminated, or changed to a higher chamber temperature.

The final group of mixtures are then compared for the value of the viscous flow parameter $\rho v/\mu$ which must be maximized. Once the mixture is established, the scaling and compression factors are determined from the viscous flow similarity rule. Use of the viscous flow relations is described in detail in section III A.

In summary then, the following outline (Table IV) shows the procedure which has been established for selecting simulants.

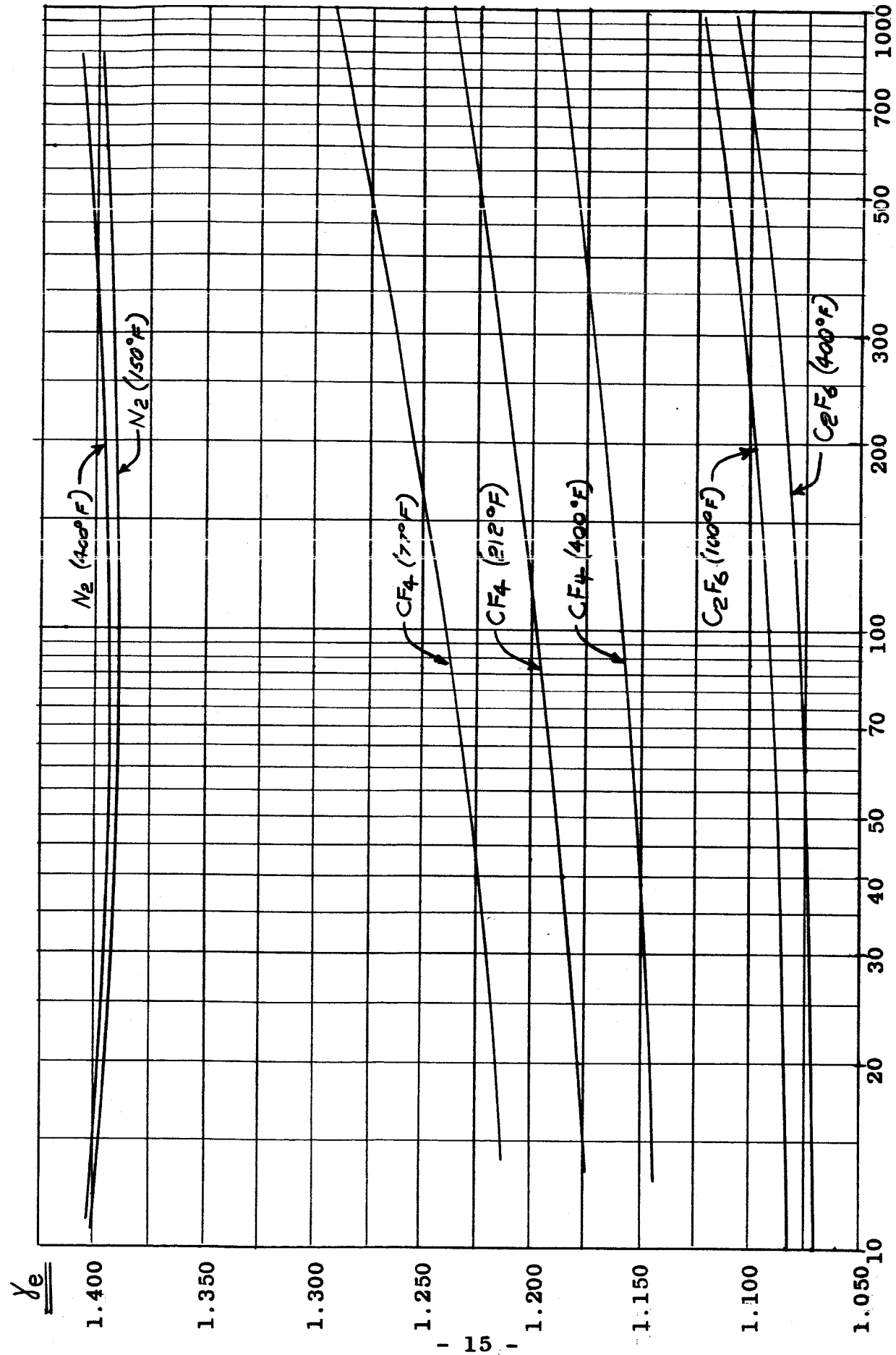

Figure 3, Exit Plane Gamma vs. P_c/P_e for N_2, CF_4 and C_2F_6

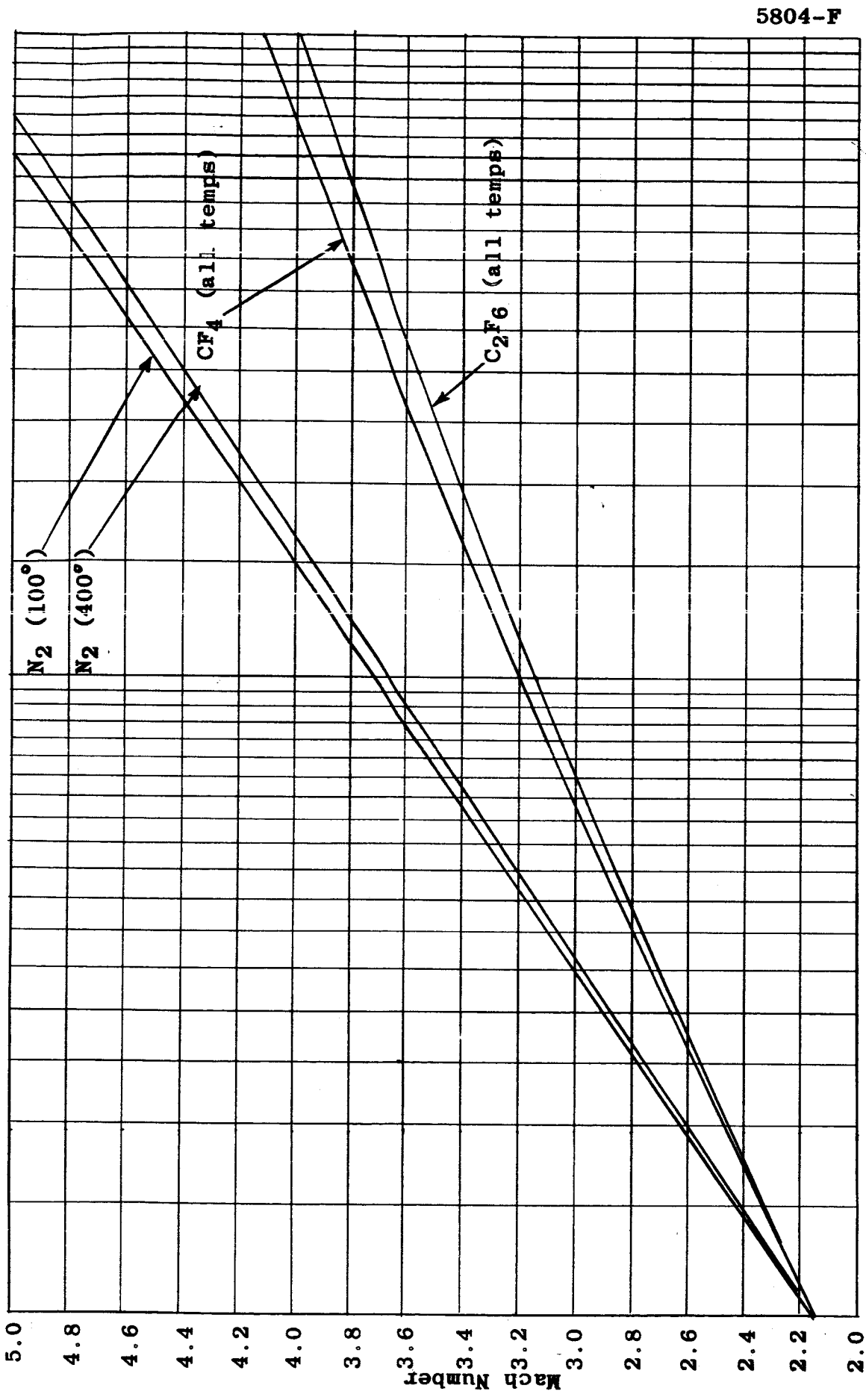

Figure 4, Mach Number vs. P_c/P_e for N_2, CF_4 and C_2F_6

TABLE IV. OUTLINE OF SIMULANT SELECTION PROCEDURE

1. Preliminary Screening.

a. All available gases surveyed (refer to Figure 2 and Table III).

b. Eliminate high boiling, toxic, high gamma, and unavailable or expensive gases.

2. Characterization.

a. Characterize remaining gases using the Simulant Characterization Program (Appendix A).

b. Plot resulting gamma, Mach number and viscous flow parameter as function of P_c/P_e and T_c.

c. Select components for mixtures which will simultaneously match gamma and Mach number.

3. Optimization of Mixture Ratios

a. Determine exact mixture ratios required for a reasonable range of P_c/P_e and T_c.

b. Eliminate range of mixtures showing possibility of condensing in the exhaust.

c. Select the mixture having the maximum viscous flow parameter from the remaining mixtures.

C. Properties and Rating of Candidates

A search of the technical literature dealing with large-molecule gas thermodynamic properties has yielded important information on the thermodynamic properties of many fluorocarbons and other gases.

The principal candidates are the low-boiling fluorocarbons and CO_2. Since the gamma of CO_2 is on the high end of the range of interest it was excluded from consideration, as either a diluent or a simulant, due to the better Mach number and boiling point of nitrogen. The fluorocarbons are of the same form as hydrocarbons with fluorine, and sometimes chlorine or bromine atoms in place of some or all of the hydrogen atoms (Refer to Figure 2). For example, for the 5-atom configurations, four atoms in any combination of fluorine, chlorine, bromine or hydrogen can combine with a carbon atom. The important candidates have been listed and are shown in Table III.

Figure 1 shows the vapor pressures of a number of these gases as a function of temperature. In addition to the computor program discussed in the previous section, Appendix B gives the properties and performance of several of the simulant candidates. Since these gases are known by several trade names such as "Freon" and "Genetron", they will be referred to by their chemical formula to avoid confusion. Ratings have been applied to these candidates to indicate the extent of our knowledge of their properties, their applicability to simulation, and cost. Table V illustrates the compounds, the hydrocarbons from which they are derived, and their ratings as simulants.

The gases which have been thoroughly characterized and remain under consideration as simulant ingredients are listed below, along with their common trade names.

CF_4	Freon 14
CHF_3	Freon 23
$CClF_3$	Freon 13
$CBrF_3$	Freon 13B1
C_2F_4	Tetrafluoroethylene
$CHClF_2/C_2ClF_5$	Freon 502
$C_2H_2F_2$	Vinylidene Fluoride
C_2F_6	Freon 116

TABLE V

RATING OF VARIOUS FLUOROCARBON SIMULANT CANDIDATES

(Ratings: 0=Unsuitable, 1=Barely Suitable, 2=Moderately Suitable 3=Excellent)

No. of Atoms	Hydro-carbons	Fluoro-carbons	Simulation Capability	Certainty of Data	Cost
5	CH_4	CF_4	3	3	1
		CHF_3	2	3	1
		CH_2F_2	1	1	0
		$CClF_3$	2	3	1
		CCl_2F_2	0	3	2
		$CBrF_3$	1	1	2
		$CHClF_2$	0	2	3
		CH_3Cl	0	1	0
6	C_2H_4	C_2F_4	2	1	2
		$C_2H_2F_2$	3	2	3
8	C_2H_6	C_2F_6	2	1	2
		C_2ClF_5	0	2	2
Azeotropic Mixture		$CHClF_2/C_2ClF_5$	1	1	2

The gases listed above have been found to exhibit properties which make them all possible simulant candidates, depending on the actual propellant system to be simulated, and the degree of size scaling required. The complete analysis of the properties indicates that of these gases, CF_4 and C_2F_6, when mixed with nitrogen, will form mixtures covering the range of gammas and Mach numbers of primary interest. (That is, gammas between 1.15 and 1.30 and Mach numbers between 3 and 4 at reasonable pressure ratios). Binary mixtures will also cover this range of gammas and Mach numbers if chamber temperature is adjusted. Ternary mixtures, however, enable chamber temperature to be adjusted solely on the basis of condensation and viscous flow considerations.

III. GAS MIXTURE AND NOZZLE OPTIMIZATION

A. Viscous Flow Requirements

Study of the viscous flow similitude rule indicates that the length should be scaled down more than the diameter, indicating that the contour may have to be compressed. The viscous flow similitude rule is expressed as:

$$\frac{d_M}{d_A}\sqrt{\frac{X_A \mu_A \rho_M v_M}{X_M \mu_M \rho_A v_A}} = 1 \qquad (1)$$

We define the model nozzle compression factor as:

$$K_M = \frac{X_M d_A}{d_M X_A} \qquad (2)$$

substituting $K_M d_M/d_A$ for X_M/X_A in (1) and squaring both sides yields:

$$\frac{\rho_M v_M \mu_A d_M}{\rho_A v_A \mu_M d_A} = 1 \qquad (3)$$

This rule will be satisfied by constructing a model with a suitable characteristic length X_M, after maximizing the quantity $(\rho_M v_M/\mu_M)$ by selecting the additive simulant. Indications are that such compression can take place to a moderate extent without disrupting smooth expansion. The minimum practical compression factor has been estimated as approximately 0.30 to 0.35. The maximum practical value of d_M/d_A is believed to be .030.

The actual contour of the engine to be simulated is a relatively long bell-shaped nozzle. Among the conditions essential to simulating the plume shape, is one that the exit

half angle be of the proper value. A small difference may be necessary for complete matching of plume shapes by compensating for different rates of change in δ between actual and model engines.

Although the external shape must faithfully duplicate the actual engine, there is no limitation on the internal contour except that the flow should not separate or shock down to subsonic velocities.

The value of $(\rho v/\mu)$ for engines using propellants, area ratios and pressure ratios similar to the F-1 engine is approximately .0064 (g/cc) (ft/sec)/(micropoise).

In the case of the ternary mixtures (discussed in the following section), the attainable value of $(\rho v/\mu)$ is approximately .054 at P_c = 1000 psia, and .074 at P_c = 1500 psia, for a pressure ratio of 150.

It has been determined that the nozzle compression factor applies mainly to the turbine exhaust which forms the major boundary layer. The core flow does not have to meet the similitude rule exactly, unless the turbine exhaust is absent in the model. For this reason, inserting a turbine exhaust flow into the model sufficiently far downstream in the nozzle is advantageous from the standpoint of making it easier to meet the viscous flow similitude requirement in the boundary layer without compressing the nozzle unduly.

A reasonably close adherence to the viscous flow rule has been shown to be possible with the core flow. In addition, the turbine exhaust affords a means of meeting this rule with precision. Figure 5 illustrates the relationships between $(\rho_M v_M \mu_A / \rho_A v_A \mu_M)$, d_M/d_A and K_M required to satisfy the viscous flow rule. Specifically, K_M vs. the viscous flow parameter ratio is shown for several values of d_M/d_A.

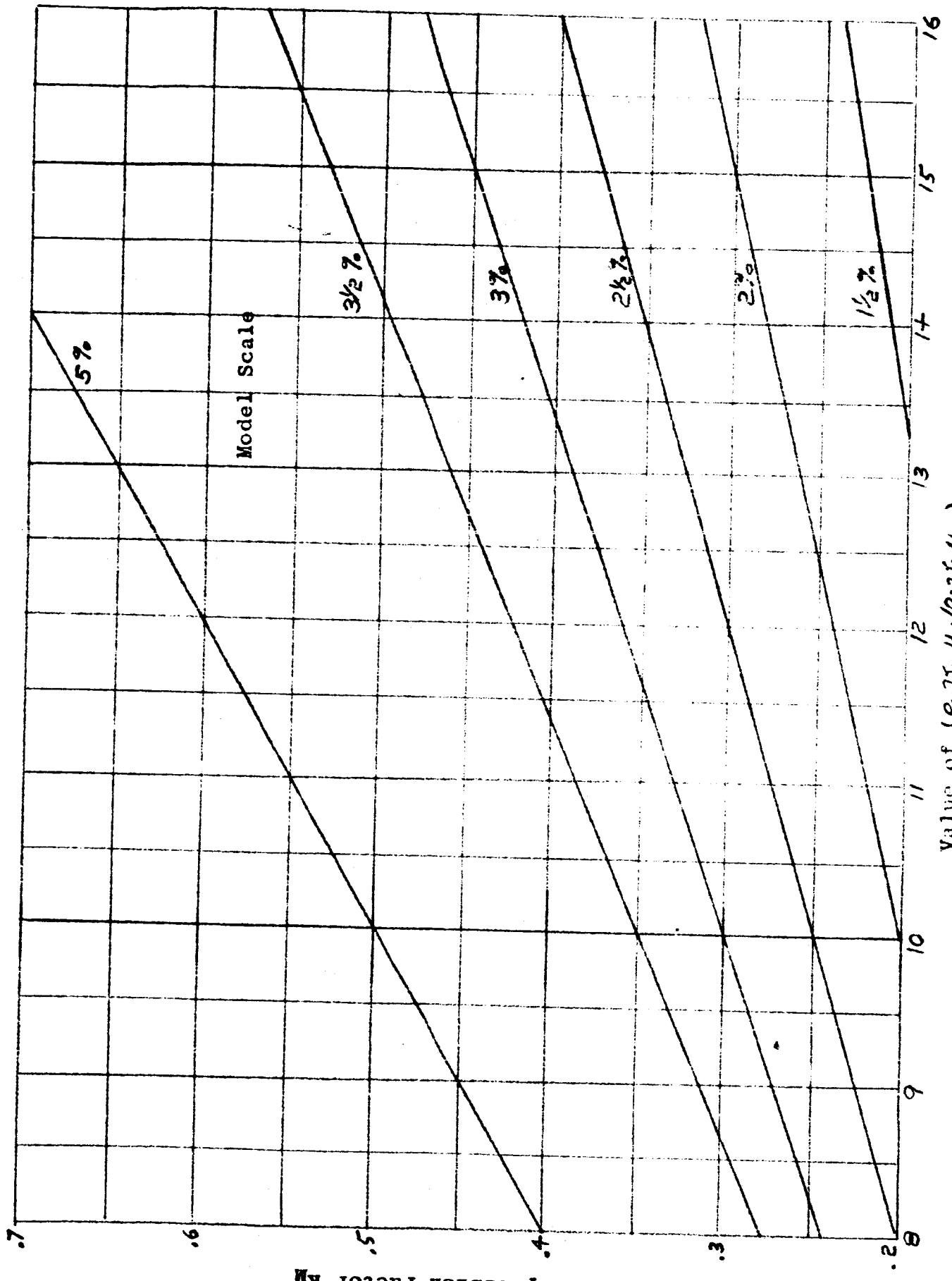

Figure 5. Nozzle Compression Vs. Viscous Flow Parameter Ratio

B. Predicted Behavior of Selected Mixtures

Simultaneous simulation of the exhaust pressure, Mach number and γ_e, can be closely approached for real engines having Mach numbers in the 3 to 5 range, using some unmixed simulants. For example, Figures 3 and 4 show that the F-1 engine, having an exhaust Mach number of 3.57, a γ_{ex} of 1.22 and P_e = 6.7 could be simulated by CF_4 at a P_c/P_e ratio of approximately 208, and a chamber temperature of approximately 176 degrees F. These values are in the mid-range of the RP-1/LOX data obtained from NASA.

As a result of carrying out the selection process outlined in the preceeding section, ternary mixtures of CF_2, C_2F_6 and N_2 were chosen and further investigated analytically for their ability to meet the similitude requirements of the F-1 engine model. It has been found that the mixtures will exactly match gamma and Mach number simultaneously. Tables VI and VII show M_e, γ_e and $\rho v/\mu$ for various pressure ratios with chamber pressures of 1000 and 1500 psia, respectively. The higher chamber temperature in the 1500 psia cases reflects an attempt to keep the temperature—pressure relationship parallel to the vapor pressure curves shown in Figure 1. The triangular contour plots in Figures 6 and 7 show constant γ and constant M_e curves for these mixtures.

Viscous flow similitude is met with these mixtures only in relatively large scale nozzles with considerable compression (See Figure 5.) As a result, it is advisable here to use the turbine exhaust as a device to meet viscous flow similitude without nozzle compression as described in the preceeding section.

At extremely high altitudes and Mach numbers, the wind tunnel atmosphere may be below the condensation temperature of C_2F_6. When this occurs it is eliminated, requiring a higher chamber temperature to meet gamma and correspondingly poorer viscous properties. Proper placement of the turbine exhaust may alleviate this problem. Under these conditions neat CF_4 or a mixture containing a small percentage of nitrogen would be used.

TABLE VI

PERFORMANCE OF TERNARY MIXTURES AT P_c = 1000 psia, AND T_c = 80°F, FOR VARIOUS EXIT PRESSURES

Ingredients, % b.w. CF_4	C_2F_6	N_2	P_c/P_e	P_e psia.	Mach No.	$\overline{\gamma}$	$\rho_e v_e/\mu_e$
17	50	33	150	6.667	3.53	1.240	0.0517
17	48	35			3.54	1.246	0.0532
17	46	37			3.56	1.253	0.0547
15	50	35			3.54	1.244	0.0529
19	46	35			3.54	1.249	0.0536
37	41	22	175	5.714	3.55	1.223	0.0465
37	39	24			3.57	1.230	0.0480
37	37	26			3.58	1.238	0.0475
35	41	24			3.56	1.228	0.0474
39	37	24			3.57	1.233	0.0484
55	33	12	200	5.000	3.57	1.204	0.0413
55	31	14			3.58	1.212	0.0428
55	29	16			3.59	1.221	0.0397
53	33	14			3.58	1.210	0.0425
57	29	14			3.58	1.215	0.0431

TABLE VII

PERFORMANCE OF TERNARY MIXTURES AT P_c = 1500 psia, AND T_c = 115°F FOR VARIOUS EXIT PRESSURES

Ingredients % b.w. CF_4	C_2F_6	N_2	P_c/P_e	P_e psia	Mach No.	$\overline{\gamma}$	$\rho_e v_e/\mu_e$
37	40	23	175	8.571	3.55	1.220	0.0626
37	38	25			3.56	1.228	0.0628
37	36	27			3.58	1.235	0.0647
35	40	25			3.56	1.225	0.0625
39	36	25			3.56	1.230	0.0632
55	32	13	200	7.500	3.56	1.201	0.0545
55	30	15			3.58	1.209	0.0564
55	28	17			3.59	1.218	0.0566
53	32	15			3.57	1.207	0.0560
57	28	15			3.58	1.212	0.0569
75	23	2	225	6.667	3.56	1.175	0.0488
75	21	4			3.57	1.184	0.0492
75	19	6			3.59	1.194	0.0512
73	23	4			3.57	1.182	0.0489
77	19	4			3.58	1.187	0.0496

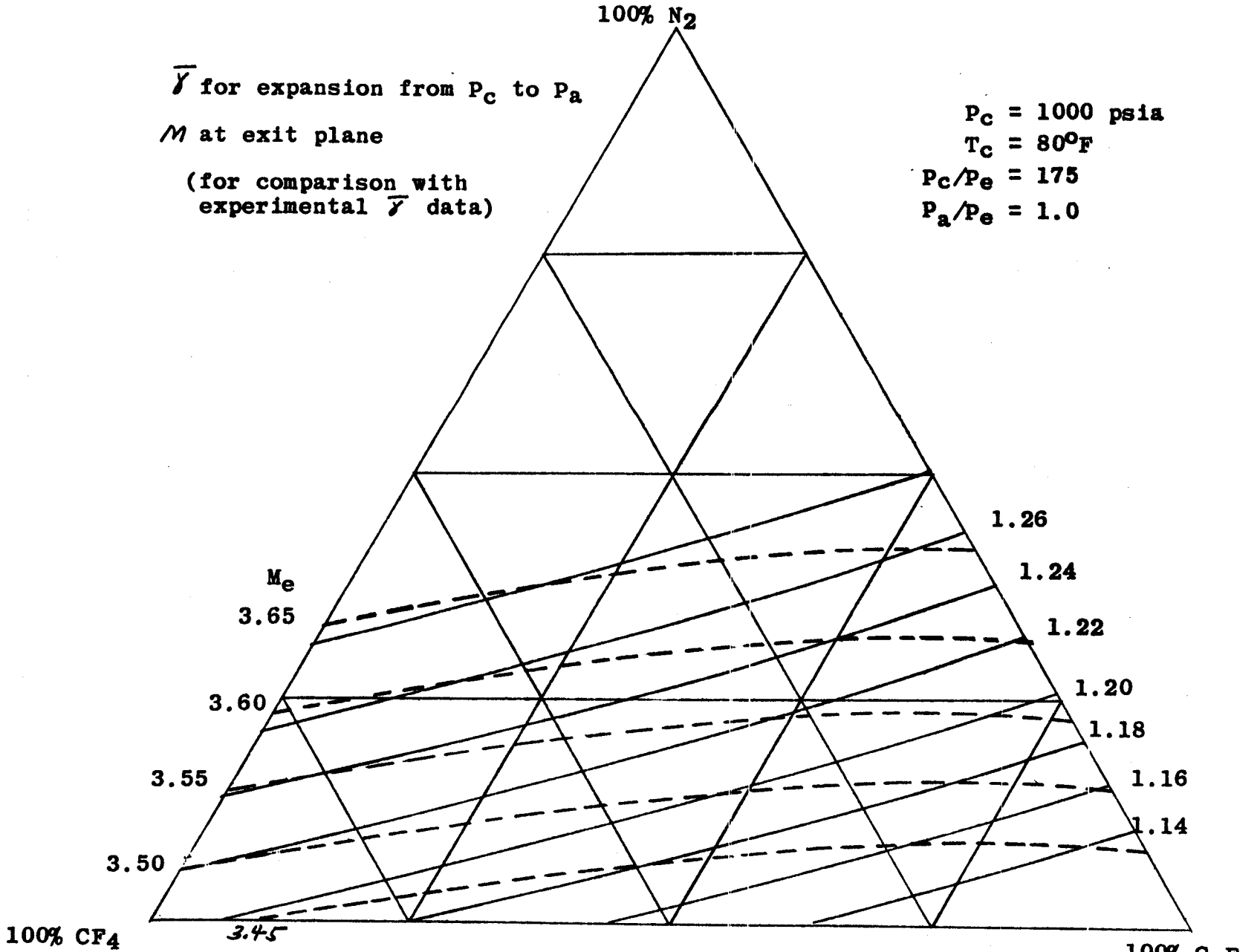

Figure 6. Constant Gamma and Mach Number Contours For $CF_4/N_2/C_2F_6$ Mixtures

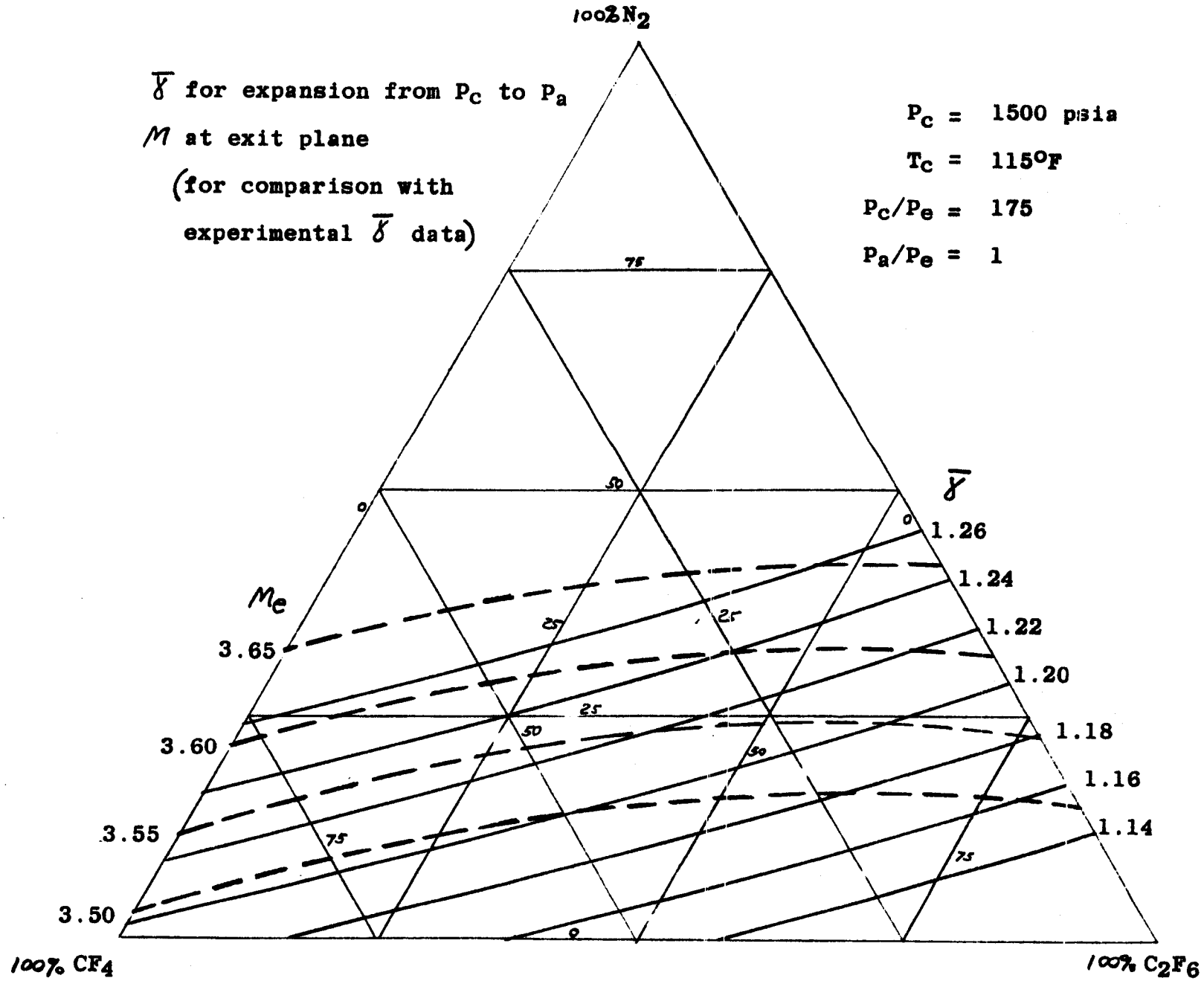

Figure 7. Constant Gamma and Mach Number Contours For $CF_4/N_2/C_2F_6$ Mixtures

C. Nozzle and Turbine Exhaust Inlet Requirements

The exact contour of the nozzles of most actual engines is a relatively long bell-shape. Among the conditions essential to simulating the plume shape, is one that the exit half angle, θ_n, be of the proper value. For simulation of the F-1 engine θ_n must be approximately equal to the 10-degree divergence of the actual engine. A small difference may be necessary for complete matching of plume shapes by compensating for different rates of change in γ between actual and model engines.

Although the external shape must faithfully duplicate the actual engine, there is no limitation on the internal contour except that the flow should not separate or shock down to subsonic velocities.

Study of the viscous flow similitude indicates that the length should be scaled down more than the diameter, to reduce boundary layer build-up, indicating that the contour may either have to be compressed or the turbine exhaust brought in further downstream. Indications are that compression can take place to only a moderate extent without disrupting smooth expansion. Figure 8 illustrated various degrees of compression.

At the high altitude and high Mach number conditions mentioned earlier, the boundary layer thickness must be controlled through placement of the turbine exhaust inlet. The area ratio where the turbine exhaust enters the F-1 engine nozzle is approximately 10. The distance between this inlet and the exist plane (ϵ = 16) must be reduced in direct proportion to the required nozzle compression factor. Thus, a factor of 0.3 leads to placement of the turbine exhaust at ϵ = 14, and a factor of 0.15 leads to placement of the turbine exhaust at ϵ = 15.

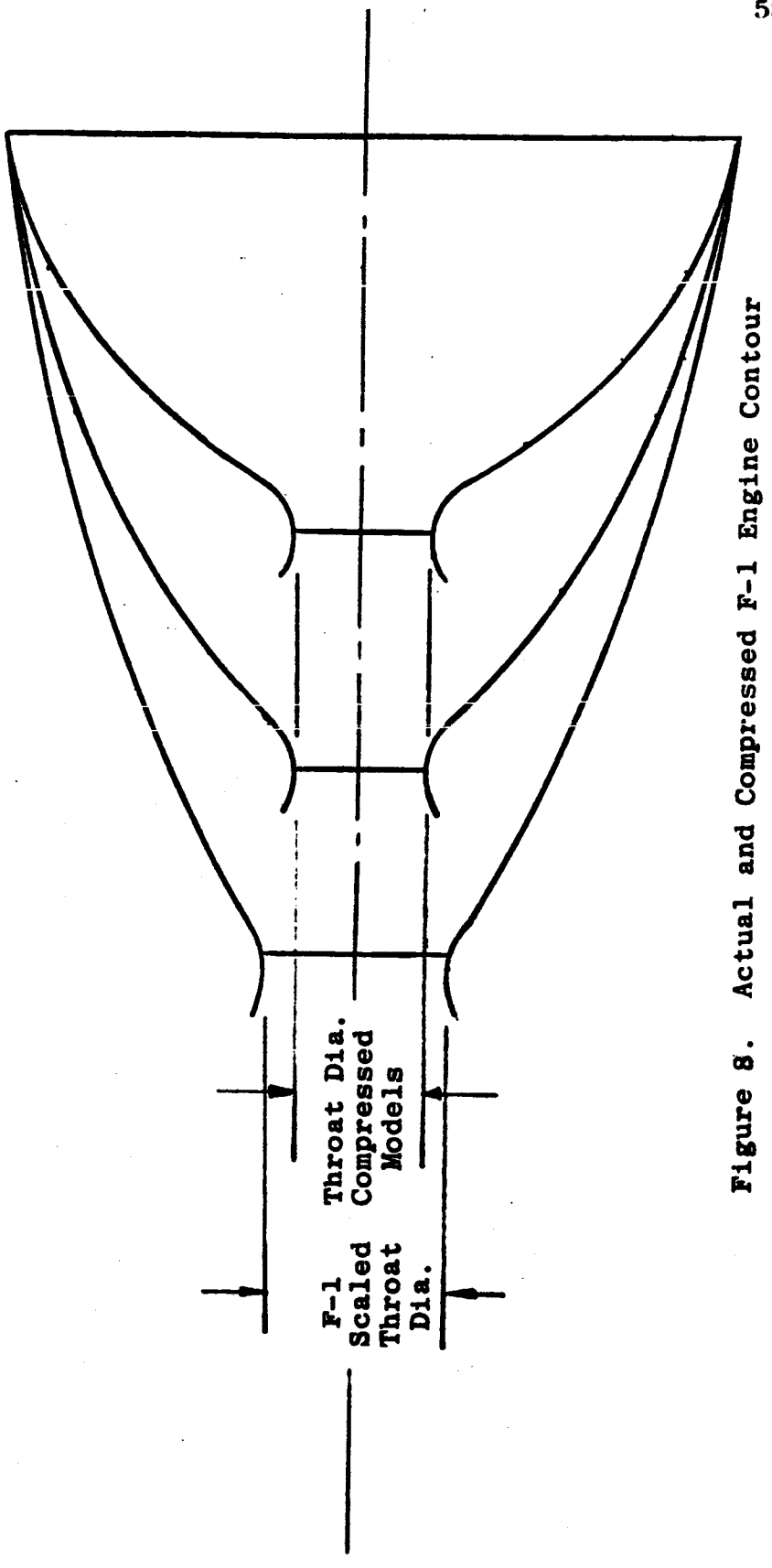

Figure 8. Actual and Compressed F-1 Engine Contour

IV. EXPERIMENTAL APPARATUS AND PROCEDURE

A. Apparatus Design and Description

The apparatus was designed to provide a steady state flow of gas for up to 3 seconds at a chamber pressure of 1000 psia, through a 1/2-inch diameter nozzle throat.

An analog simulation of the contemplated apparatus was prepared and used in the design of the system. Of particular importance was the design of the heater which was used to heat the simulants. Flow tests with nitrogen gas were made to determine the behavior of the apparatus. Operation was analyzed and found to be satisfactory and in good agreement with the analog computer results. The analog computer program equations including a block diagram of the computer circuitry appear in Appendix C. Table VIII shows the parameters given by the analog program for the heater one second after the valve opens.

The apparatus was assembled in Test Stand 2A in Thiokol-RMD's Test Area A. The test stand consists of a firing bay housing the apparatus, and a control room which houses a control console and strip chart recorders. A central instrumentation building is located within the area and services the test stand with high-speed recording equipment. Also provided within the area is a high pressure, regulated, nitrogen gas cascade system. The nitrogen system has been used to check out the test setup and provides the high pressure nitrogen required for some of the testing.

The test setup for the evaluation of simulant gas mixtures consists of a high pressure reservoir, pressure regulator, upstream valve, heater, prop valve (downstream) chamber, and nozzle. System design parameters are 2190 psig tank working pressure, 20 lb/sec maximum gas flowrate and 1150 psig chamber pressure. Figure 9 is a schematic diagram of the apparatus. Figure 10 is a photograph of the completed setup installed in the test bay.

The run tank consists of a carbon steel tank fabricated from standard heavy wall tubing components. Heating elements surrounding the tank are used to electrically heat the gas mixture in the tank to prevent condensation of the simulants in the pressure regulator and to reduce the required size of the downstream heater. The run tank has a volume of 4.925 cubic feet and has a maximum working pressure of 2190 psig at 650°F. The tank has been hydrotested at 3280 psig. The tank temperature capability provided by the strip heaters is 250°F. The outer surface of the reservoir has

TABLE VIII

TYPICAL OPERATING PARAMETERS OF THE HEATER AFTER ONE SECOND OF OPERATION

*	Total weight of balls	420 lbs.
*	Diameter of balls	0.500 in.
*	Run tank initial pressure	2000 psia
*	Run tank temperature	212°F
*	Plenum chamber volume	0.2 ft^3
*	Inlet gas pressure	1000 psia
	Inlet gas temperature	89°F
*	Initial Heater Temperature	700°F
	Temperature, First Node	694.6°F
	Temperature, Last Node	699.5°F
*	Electrical power input	15 kw
	Outlet gas pressure	994 psia
	Outlet gas temperature	605°F
*	Valve opening time	0.4 sec.
	Time to reach steady state (approx.)	0.5 sec.

---

*Initial conditions. All other conditions are results at one second.

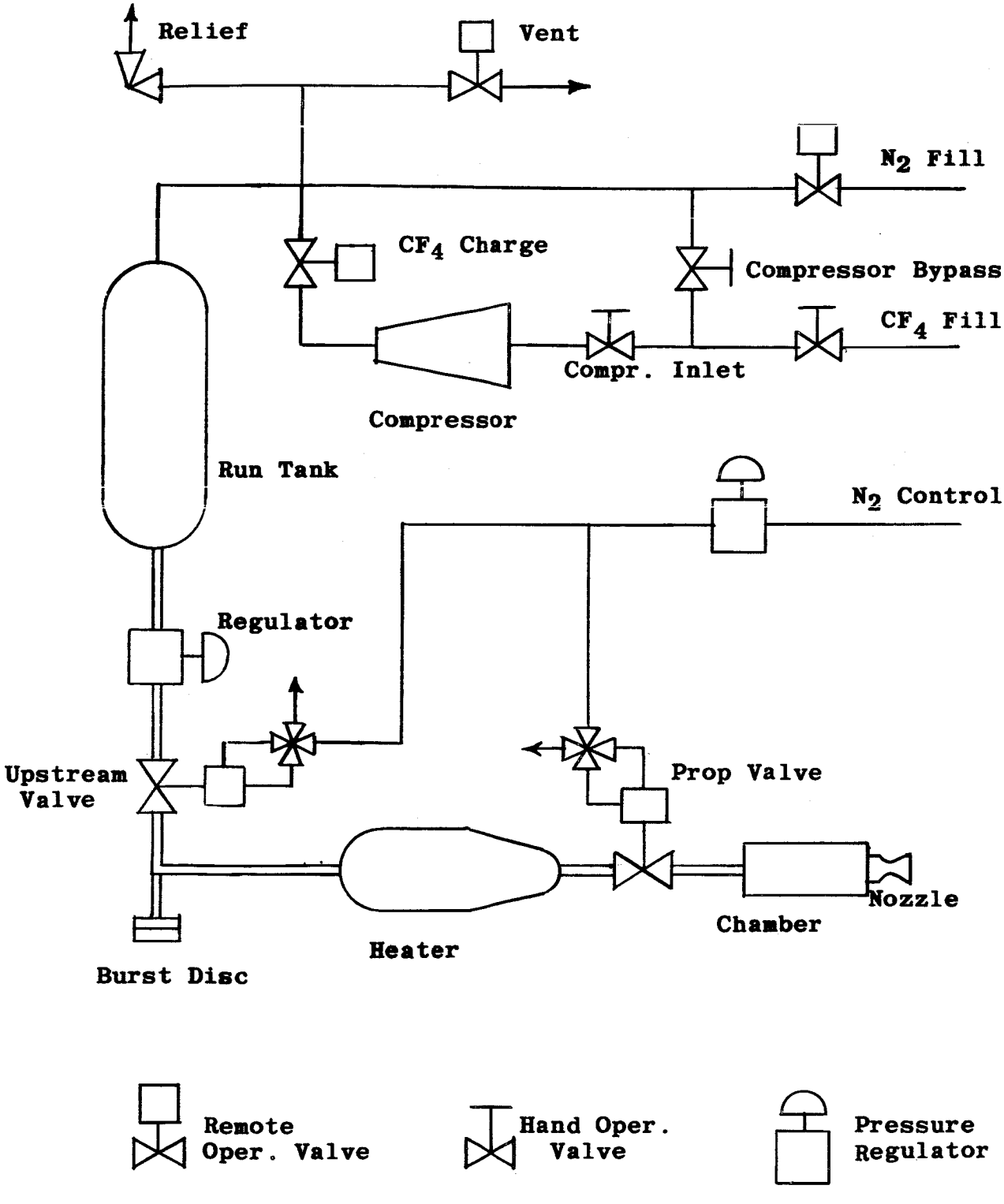

Figure 9. Schematic Diagram of Apparatus

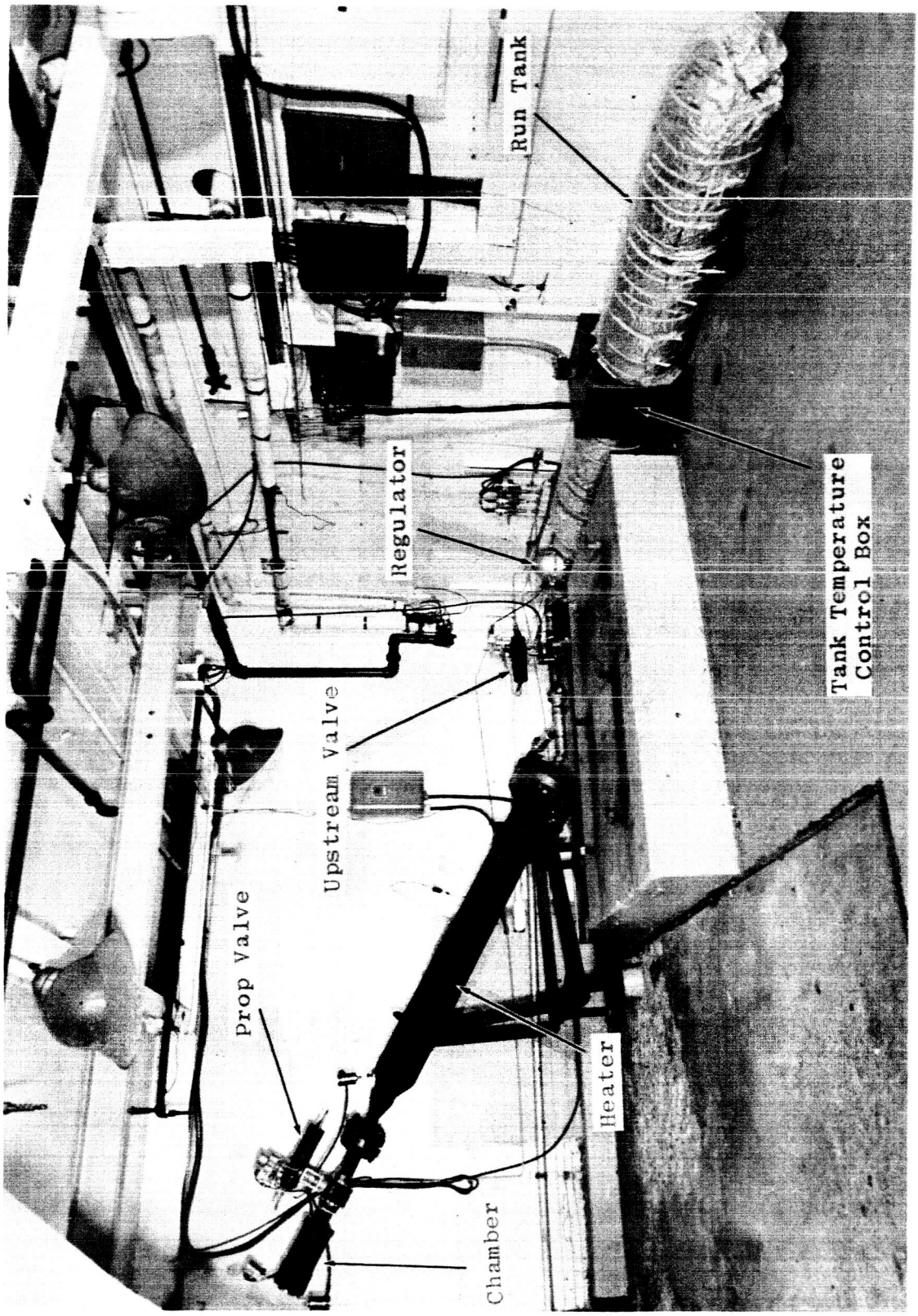

Figure 10. Photograph of Apparatus

been insulated to maintain the desired temperature of the gas mixture during testing. A thermostat ranging from 0-250°F was installed to control the reservoir's temperature.

The 2-inch ball valves, manufactured by W.K.M. Industries Inc. have a rated pressure of 1500 psig and temperature of 350°F. The valves contain teflon seats and seals. These valves are operated by pneumatic actuators. The opening and closing times have been reduced to approximately 0.4 seconds with an actuator pressure of 150 psig and a 3/8 inch feed line.

The pressure reducing regulator is of the balanced pressure type, manufactured by the Grove Regulator Company. The regulator has a maximum inlet pressure of 3500 psig and an outlet pressure of 1500 psig with a minimum pressure drop of 50 psig. The minimum inlet and outlet pressures are 100 and 50 psig, respectively. The maximum operating temperature of the regulator is 300°F.

The downstream gas heater is a pebble bed type containing 1/2 inch diameter steel balls which are preheated by tubular electric heaters. The effective heater length is 60 inches and its interior diameter is 6.625 inches. The weight of the steel balls is approximately 420 pounds. The six tubular heater rods immersed in the balls are thermostatically controlled and are capable of preheating the balls to a maximum of 650°F. The maximum working pressure of the heater is 1350 psig at 650°F. However, a 350°F working temperature limit has been imposed on the heater by the downstream prop valve seal and seat material. The heater has a potential temperature capability of 1000°F at lower pressures. The heater is capable of heating the gas to within 50°F of the ball temperature. The chamber temperature rises to this temperature in approximately 3 seconds with the large plenum chamber and 1 second with the smaller chamber. A cutaway view of the heater is shown in Figure 11.

Two chambers were designed and fabricated for the program. One was a large cylindrical plenum chamber designed to insure adequate settling of the gas. This chamber was flanged at both ends for attachment to the prop valve and attachment of the nozzle. Allowances were made to accommodate different nozzle configurations without any changes in the chamber itself. The small chamber was designed when it was found necessary to reduce the chamber temperature rise time. The volumes of the two chambers are 0.1 ft^3 and 0.01 ft^3, respectively. A cutaway view of the large chamber is shown in Figure 12.

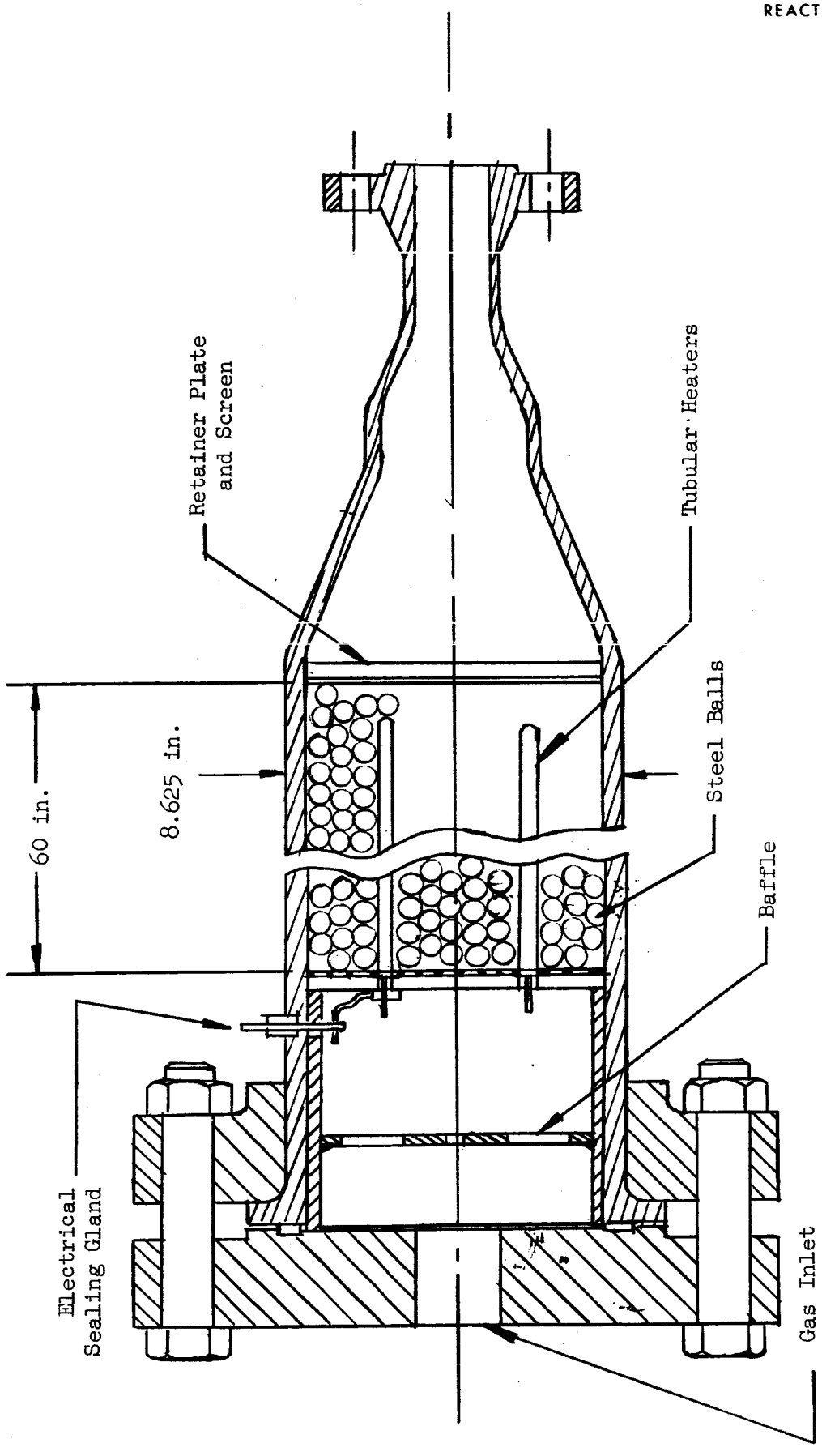

Figure 11. Cutaway View of Heater

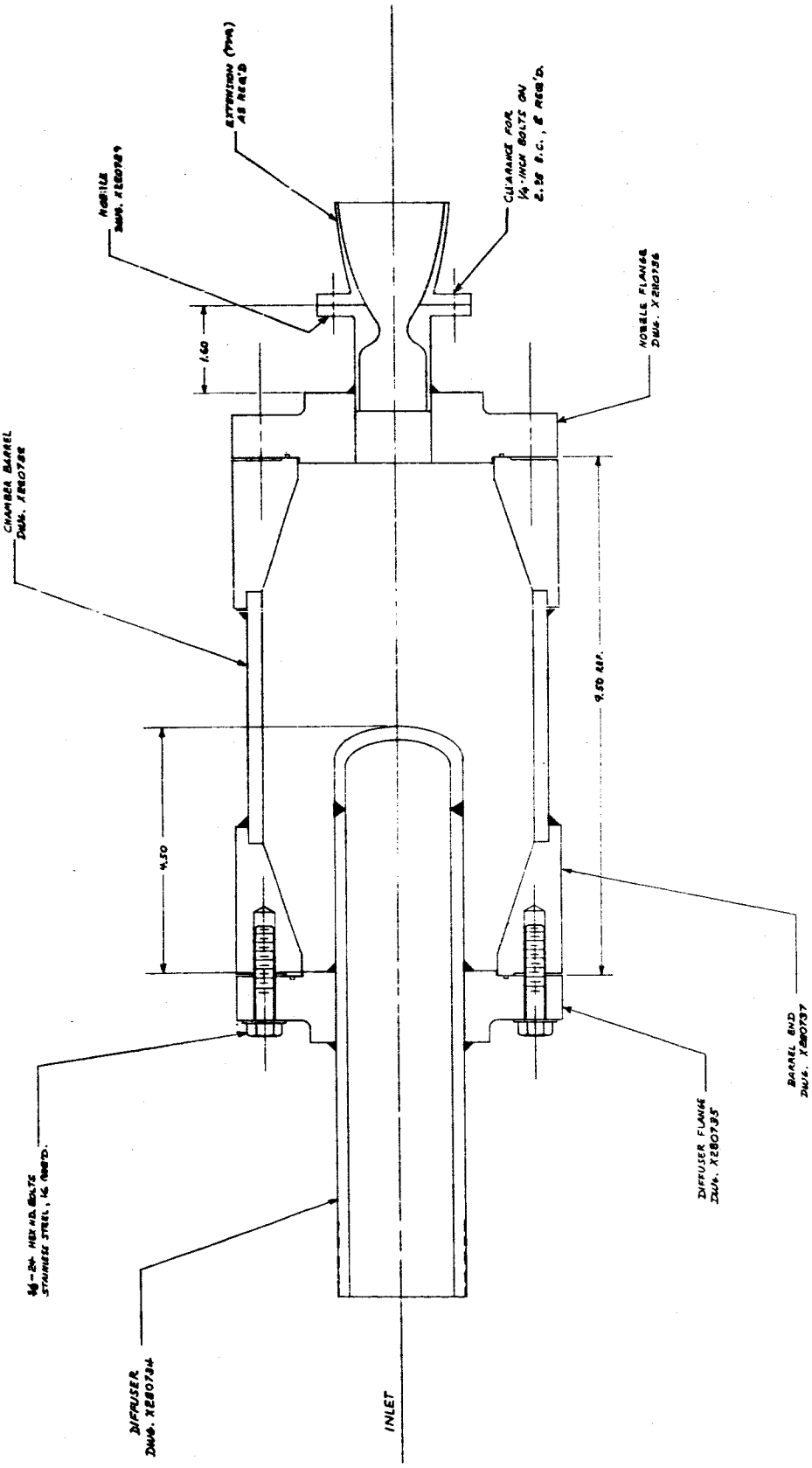

Figure 12, Cutaway view of large chamber

B. Data Acquisition and Reduction

Each chamber contained two pressure taps so that the effects of gas velocity and interchanging of pickups could be observed. The taps were arranged so as one would see stagnation pressure and the other would see static pressure. The stagnation tap reading was used, initially, providing it was the highest. If the static tap read higher, the data was not used. Figure 13 shows schematically, the arrangement of pressure taps in the two chambers. (Chambers are not shown to scale, since the one with the standpipe is much larger than the smaller one.) The nozzles are also shown with their approximate static tap locations.

The chamber pressure transducers were interchanged after run 2AX-3999 on the large chamber and a difference of 2.6% was discovered between the two transducers in addition to the difference between locations. Comparison of the results with the known properties of nitrogen indicated that an average between the two transducers would give results closer than either one alone. The small difference in chamber pressure readings made a more precise correction of little value, since the error possible in reading the traces was as large as the difference between transducers. (See Section V-E.)

The conical nozzle was constructed in two sections. One section contained a pressure tap at an area ratio of 4.06 and the other contained a pressure tap at an area ratio of 9.1. Runs 3990 through 3999 were conducted with only the $\epsilon = 4.06$ nozzle section. The remaining runs (except 4015 - 4017) used both nozzle sections. Figure 14 shows a detail drawing of the conical nozzle assembly. The actual area ratios were measured after fabrication.

The data reduction procedure is outlined in Appendix D, along with an example from the test data.

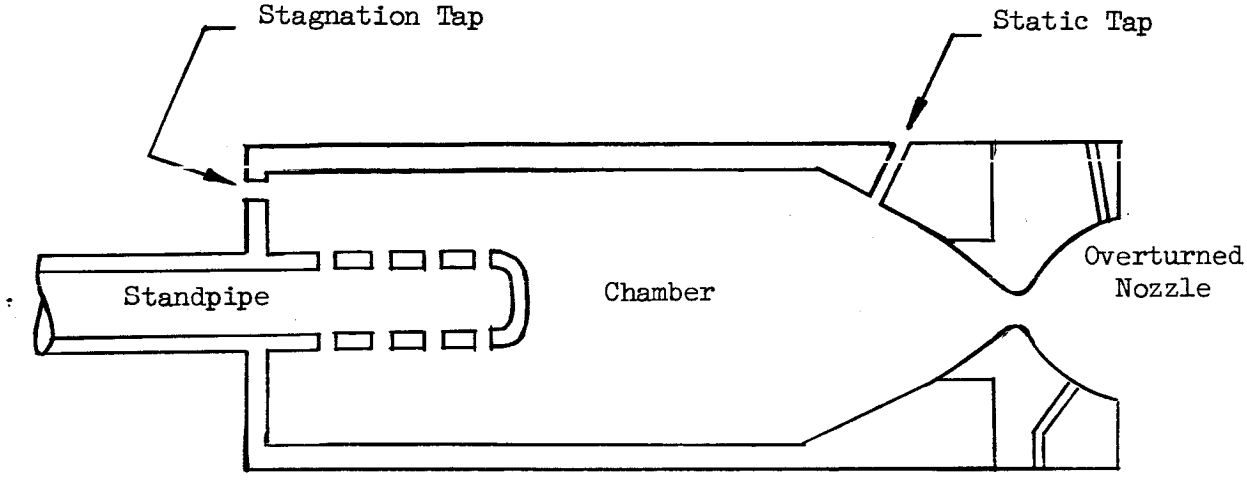

LARGE CHAMBER

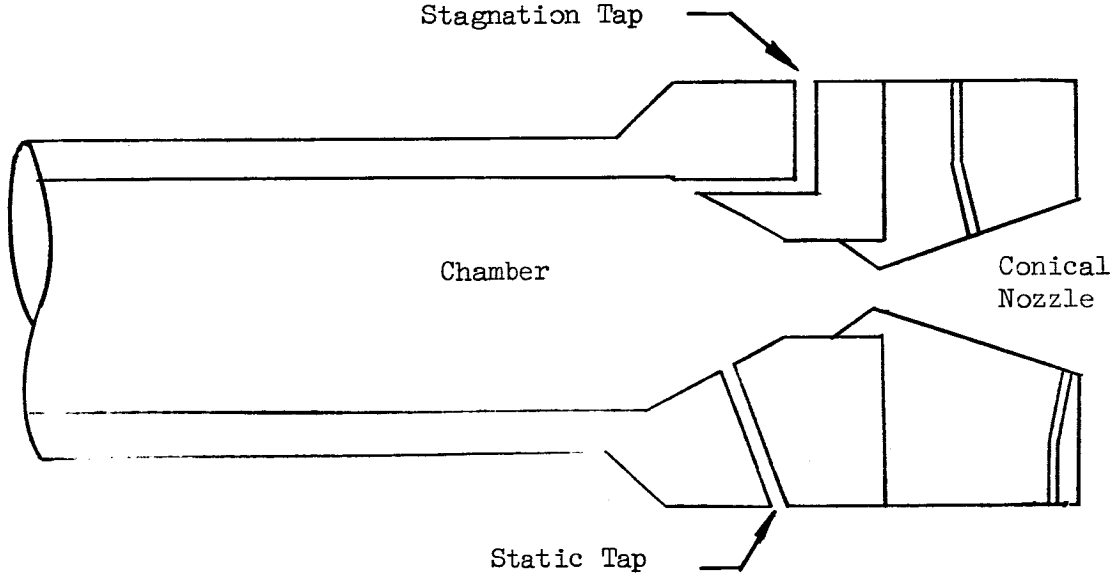

SMALL CHAMBER

Figure 13. Pressure Tap Locations

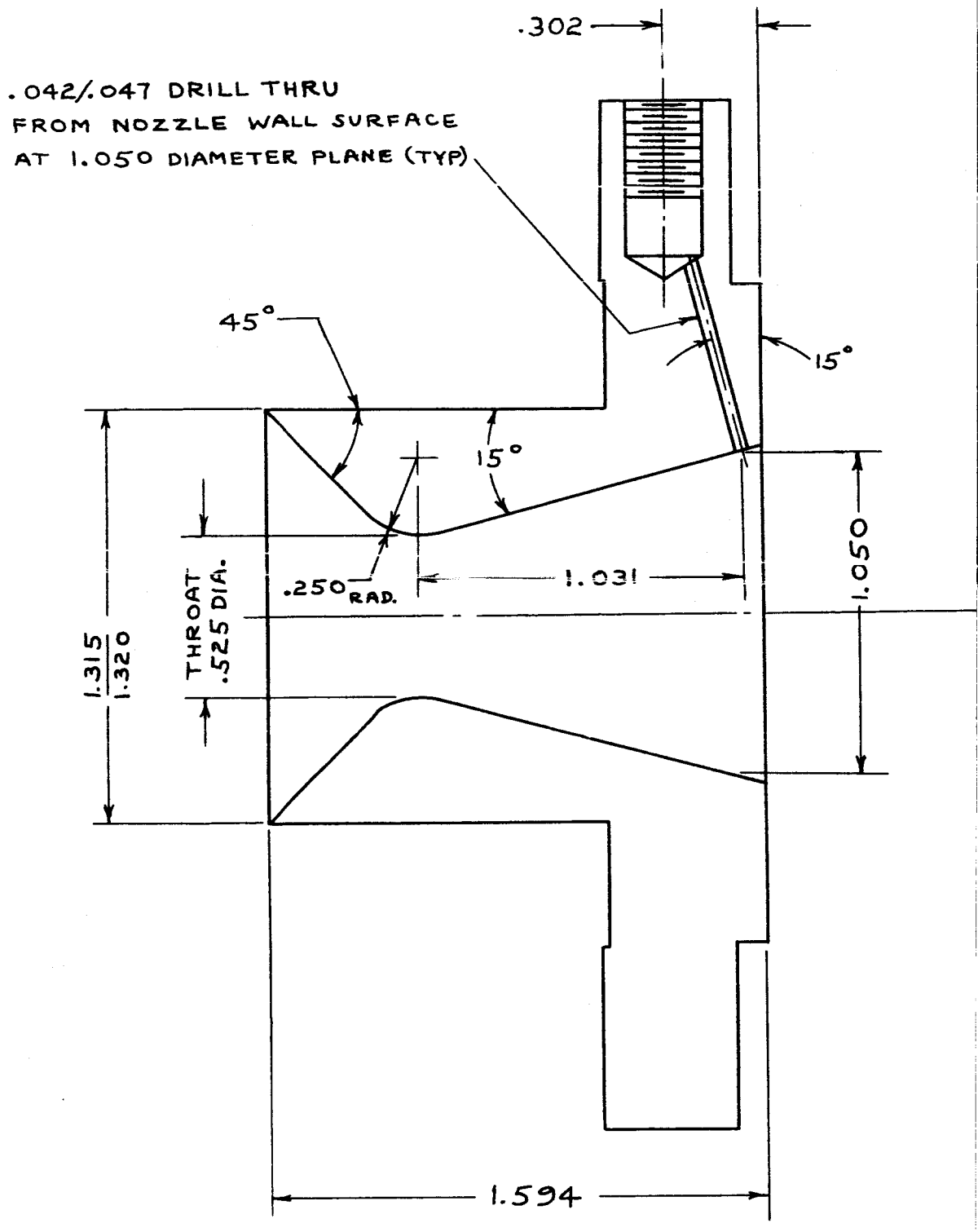

Figure 14. DETAILS

P.40 ©

Thiokol

5804-F

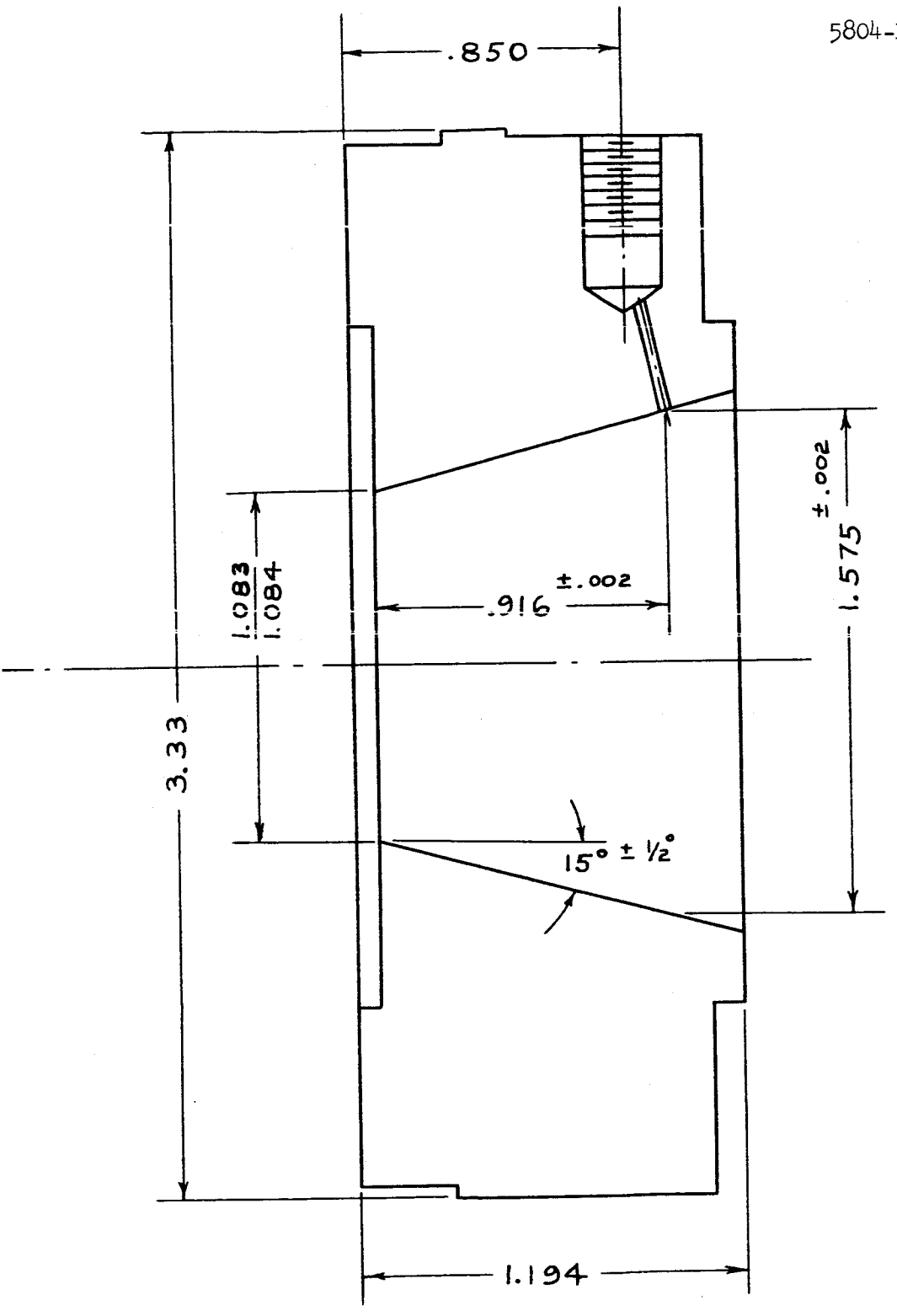

OF CONICAL NOZZLE

P.40

(2)

C. Test Program

Simulant tests were conducted in test stand 2-A to experimentally measure the effective specific heat ratio, $\overline{\gamma}$, and the pressure drop through conical and overturned bell nozzles.

The entire test program is summarized in Table IX in chronological order. Tests have been conducted with N_2, CF_4, and mixtures containing N_2, CF_4, and $CHClF_2$. Both binary and ternary mixtures were used. $CHClF_2$ was used instead of C_2F_6 since it was well-known and less expensive. It cannot be used as a simulant, however because its boiling point is too high.

The initial flow tests were made with neat N_2 to check out the apparatus. Two cylinders of $CHClF_2$ and 12 cylinders of CF_4 were consumed. A total of 44 tests were conducted.

TABLE IX

SUMMARY OF TESTS

Run Number 2 AX-	Purpose of Series	Gas used	Max. A_e/A_t	Nozzle Type	P_c Range (psia)	No. Tests Giving Valid Data
3990-95	Checkout and Calibration	N_2	4.06	Conical	660-980	5
3996-99	Preliminary Mixture (γ) Evaluation	N_2/F22*	4.06	Conical	390-820	3
4000-02	N_2 gamma	N_2	9.1	Conical	715-935	3
4003-08	CF_4 gamma	CF_4	9.1	Conical	650-1110	6
4009-10	Binary Mixtures	CF_4/N_2	9.1	Conical	600	2
4011-14	Small Chamber Calibration	N_2	9.1	Conical	950-1100	2
4015-17	Compressed Nozzle (γ) Evaluation	N_2	9.5	Bell	1000-1150	3
4018-19	CF_4 gamma	CF_4	9.1	Conical	590	2
4020-30	Binary gamma	CF_4/N_2	9.1	Conical	800-1130	10
4031-33	Ternary gamma	CF_4/N_2/F22	9.1	Conical	600-900	3

D. Experimental Procedure

Referring to the hardware schematic (Figure 9) the experimental procedure was as follows.

(1) The pebble bed heater power is turned on. All valves are initially closed.

(2) Simulants are loaded into the run tank beginning with the one at the lowest supply pressure. Loading takes place until the desired partial pressures are reached with each simulant. Pressure and temperature of the run tank contents are carefully recorded for each simulant addition.

(3) Power to run tank heaters is turned on to bring run tank to desired operating temperature.

(4) Pressure regulator is adjusted to approximately 50 psi higher than desired chamber pressure.

(5) Upstream valve bypass valve is opened to fill heater slowly.

(6) When pebble bed heater comes to approximately the desired chamber temperature, recorders are started.

(7) Run commences about 1/2 second after recorders start by opening of prop valve.

(8) At end of run, upstream valve is closed first, then prop valve, by automatic timer.

(9) Recorders are stopped; heaters are shut off.

(10) If same simulant mix is to be tested again, procedure is repeated, except step 2.

(11) If a different mix is to be run, heater is emptied by opening prop valve. The loading procedure is similar, except that the mixture already in the run tank must be taken into account when selecting desired incremental increases in partial pressures of the ingredients. After closing the prop valve, the procedure is repeated.

Tank pressure and temperature were read from strip chart recorders in the control room. During the run, the resulting chamber and nozzle conditions were recorded on high speed recorders in the central instrumentation building.

Simulants were loaded with the run tank cold and the shipping cylinders in the sun to speed the loading. The compressor was used whenever the required tank pressure exceeded the final shipping cylinder pressure. Heating the run tank provided for longer run duration by increasing the pressure, and prevented condensation from taking place in the regulator.

V. RESULTS OF TESTS

A. Nitrogen Tests

The test program proceeded in a step-by-step manner from check-out of the apparatus with nitrogen, through testing of CF_4, to testing of binary and ternary mixtures. The test program was directed toward demonstrating that our method of predicting γ is accurate. Assuming an isentropic expansion, γ can be determined by measuring area ratio (Ae/At) and pressure ratio (Pc/Pe).

Initial tests were made using nitrogen at approximately 100°F, area ratios of 4.06 and 9.1, and a range of chamber pressures from approximately 620 psia to 930 psia. Additional tests were performed with nitrogen when different chambers or nozzles were used. The original purpose of nitrogen tests was to use the "errors" resulting in these tests to correct all other tests assuming that nitrogen was known to a high degree of precision. This was not done due to the following reasons: (See sect. V-D).

1. Errors (or differences) were not completely consistent but depended on chamber configuration, area ratio and the particular calibrations in effect at the time of the test.

2. The errors were relatively small (less than 5%) for most of the gas mixtures as well as for nitrogen.

3. Some differences were found in the theoretical values of γ for nitrogen reported in the literature. The theoretical values reported for the temperature range of interest ranged from 1.39 to 1.43. The data which we used leads to a value of about 1.395 to 1.400.

The test results for nitrogen with the 15° conical nozzle are shown in Table X. A conical nozzle was chosen for most of the tests because such a nozzle gives results closer to an isentropic expansion than does a bell nozzle. Assumption of an isentropic expansion is vital to determination of gamma.

Table XI shows results for a compressed nozzle. Gamma is not reported for all of the tests since the nozzle is not isentropic. The lower Pc/Pe values and lower apparent gamma reflect a higher pressure along the wall downstream of the throat region. This is to be expected, due to the curvature. To make this nozzle give proper pressure ratios near the exit, a conical extension with a small half-angle would have to be added.

TABLE X

TEST DATA FOR NEAT NITROGEN AND CONICAL NOZZLE

Run 2AX-	P_{ch} psia	T_{ch} °F	A_e/A_t	Experimental P_c/P_e	Experimental $\bar{\gamma}$	Theoretical P_c/P_e	Theoretical $\bar{\gamma}$	Chamber Size	% Error in Gamma
3990	987	91	4.06	33.6	1.390	34.1	1.396	Large	- 0.4
	994	174		34.0	1.395	34.1	1.396		- 0.1
3991	639	90		33.5	1.388	34.1	1.396	"	- 0.6
	675	190		34.3	1.399	34.1	1.396		+ 0.2
3992	718	76		33.9	1.394	34.1	1.396	"	- 0.1
	748	140		33.9	1.394	34.1	1.396		- 0.1
3993	838	76		34.0	1.395	34.1	1.396	"	- 0.1
	875	143		34.3	1.399	34.1	1.396		+ 0.2
3994	928	76		33.7	1.391	34.1	1.396	"	- 0.4
	948	132		34.2	1.398	34.1	1.396		+ 0.1
3995	No Data							"	
4000	720	96	4.06	34.2	1.398	34.1	1.396	"	+ 0.1
	728	113		34.6	1.403	34.1	1.396		+ 0.5
	720	96	9.1	129.6	1.433	118.9	1.400		+ 2.3
	728	113		131.1	1.438	115.0	1.398		+ 2.8
4001	794	80	4.06	34.5	1.402	34.1	1.396	"	+ 0.1
	789	115		34.2	1.398	34.1	1.396		+ 0.1
	794	80	9.1	129.7	1.434	118.9	1.400		+ 2.4
	789	115		128.9	1.431	115.0	1.398		+ 2.5
4002	945	110	4.06	34.0	1.393	34.1	1.396	"	- 0.2
	945	110	9.1	130.1	1.435	116.5	1.394		+ 2.0
4011	No Data							Small	
4012	No Data								
4013	1026	161	9.1	130.9	1.437	116.9	1.396	"	+ 2.9
	974	243		128.2	1.429	116.9	1.394	"	+ 2.5
4014	1135	168	9.1	130.3	1.435	116.9	1.396	"	+ 2.8
	912	222		128.3	1.429	116.9	1.394	"	+ 2.5

TABLE XI

TEST DATA WITH NEAT NITROGEN USING A COMPRESSED NOZZLE* AND THE SMALL CHAMBER

Run 2AX-	P_{ch} psia	T_c °F	Ae/A_t	Experimental P_c/P_e	Experimental $\overline{\gamma}$	Theoretical P_c/P_e	Theoretical $\overline{\gamma}$
4015	1012	122	7.0	61.8	1.292	78.9	1.395
	1025	167		60.3		78.9	1.395
	1012	122	11.0	156.2		155.7	1.394
	1025	167		164.0		155.7	1.394
4016	1088	134	7.0	62.6		78.9	1.395
	1105	181		62.3		78.9	1.395
	1088	134	11.0	168.5		155.7	1.394
	1105	181		171.2		155.7	1.394
4017	1203	140	7.0	65.3		78.9	1.395
	1207	185		64.4		78.9	1.395
	1203	140	11.0	185.7		155.7	1.394
	1207	185		186.3		155.7	1.394

---

*Compression factor equals approximately 0.25.

The average values of gamma for the conical nozzle and the average errors are shown below. The error is within the scatter and expected error, but there is a significant positive trend at ϵ =9.1 which may be due to an improper diameter measurement, to faulty calibration of the instrumentation, or to a higher dependence of γ on temperature.

ϵ = 4.06	Average	$\overline{\gamma}$ = 1.3958
	Theoretical	$\overline{\gamma}$ = 1.3960
	Error	= -.015%
ϵ = 9.1	Average	$\overline{\gamma}$ = 1.433
	Theoretical	$\overline{\gamma}$ = 1.397
	Error	= +2.51%

B. Neat CF_4 Tests

Tests performed with neat CF_4 show a similar trend to a higher $\overline{\gamma}$ at $\epsilon = 9.1$. This time, however, the theoretical values also have some trend in this direction. This is to be expected, since the high area ratio leads to a lower temperature, which in turn leads to a higher γ and $\overline{\gamma}$.

The results are tabulated in Table XII. There is a general tendency for $\overline{\gamma}$ to be slightly higher than the theoretical value. The amount of error, however, is too small to justify changes in the properties data for neat CF_4. The average values of gamma and the differences are shown below:

$\epsilon = 4.06$	Average $\overline{\gamma}$	= 1.1813
	Theoretical $\overline{\gamma}$	= 1.1788
	Error	= +0.21%
$\epsilon = 9.1$	Average $\overline{\gamma}$	= 1.1999
	Theoretical $\overline{\gamma}$	= 1.1897
	Error	= +0.86%

TABLE XII

TEST DATA FOR NEAT CF_4 IN THE CONICAL NOZZLE

Run 2AX-	P_{ch} psia.	T_{ch} °F	A_e/A_t	Experimental P_c/P_e	Experimental γ	Theoretical P_c/P_e	Theoretical γ	Chamber Size	% Error in Gamma
4003	1072	98	4.06	22.6	1.180	23.1	1.180	Large	0
	1091	117		22.7	1.181	22.6	1.175	"	+ 0.5
	1072	98	9.1	71.0	1.203	68.5	1.190	"	+ 1.0
	1091	117		71.7	1.206	67.8	1.185	"	+ 1.8
4004	1131	96	4.06	23.0	1.189	23.1	1.180	"	+ 0.8
	1118	104		23.0	1.189	22.9	1.178		+ 0.9
	1131	96	9.1	72.5	1.211	68.3	1.191		+ 1.7
	1118	104		72.2	1.209	23.5	1.190		+ 1.5
4005	656	77	4.06	23.3	1.197	23.5	1.186	"	+ 0.9
	658	96		23.1	1.191	23.1	1.180		+ 0.9
	656	77	9.1	71.3	1.204	70.2	1.198		+ 0.5
	658	96		71.5	1.205	69.4	1.193		+ 1.0
4006	1046	98	4.06	22.1	1.170	23.1	1.180	"	- 0.8
	1050	120		22.4	1.178	22.6	1.174		+ 0.3
	1046	98	9.1	68.8	1.192	68.8	1.192		0
	1050	120		69.6	1.195	61.5	1.184		+ 0.9
4007	856	84	4.06	22.7	1.182	23.4	1.183	"	- 0.1
	853	115		22.8	1.185	22.8	1.175		+ 0.8
	856	84	9.1	71.3	1.204	69.3	1.194		+ 0.8
	853	115		70.3	1.199	67.3	1.186		+ 1.0
4008	937	98	4.06	22.2	1.171	23.1	1.180	"	- 0.8
	945	124		21.9	1.166	22.5	1.173		- 0.6
	937	98	9.1	71.9	1.208	68.5	1.190		+ 1.5
	945	124		68.5	1.190	69.3	1.183		+ 0.6
4019	594	100	4.06	22.5	1.178	23.1	1.180	Small	- 0.2
	594	100	9.1	67.8	1.186	68.5	1.190	"	- 0.4

C. Tests of CF_4/N_2 and $CF_4/CHClF_2/N_2$ Mixtures

Of the 9 tests conducted with CF_4/N_2 mixtures, 8 yielded useful data. There was a trend toward a positive error, particularly in the $\epsilon = 9.1$ cases. The average error or difference in gamma for the $\epsilon = 4.06$ cases was +0.73% with a scatter of 4.7%. The average error for the $\epsilon = 9.1$ cases was + 1.70% with a scatter of 3.3%. (The scatter for the $\epsilon = 4.06$ cases does not include a point with a 4.4% error and the scatter in the $\epsilon = 9.1$ cases does not include a point with a -1.1% error). Table XIII shows the experimental data for these mixtures.

Figures 15 and 16 illustrate the variation in gamma with mixture ratio for the $\epsilon = 4.06$ and the $\epsilon = 9.1$ cases, respectively. The experiments with neat gases shown at the edges were run with chamber temperatures near 100°F indicating the gamma values shown. The mixtures had chamber temperatures between 100 to 264°F, with most temperatures between 150 and 250°F. The lower gammas expected with the higher temperatures are reflected by the triangular (calculated) points. The vertical shaded bands indicate the range of the experimental points (except those excluded in determining the scatter). The straight line approximations, indicated by the thin lines, are assuming the chamber temperature remained in the neighborhood of 100°F.

TABLE XIII

TEST DATA FOR N_2/CF_4 MIXTURE USING CONICAL NOZZLE

Run 2AX	% N_2	% CF_4	P_{ch} psia	T_{ch} °F	A_e/A_t	Experimental P_c/P_e	Experimental $\overline{V}_0$	Theoretical P_c/P_e	Theoretical $\overline{V}_0$	% Error in Gamma
4009*	71.0	29.0	903	100	4.06	29.65	1.321	28.8	1.305	+ 1.2
			810	147		30.22	1.331	28.4	1.298	+ 2.5
			903	100	9.1	106.3	1.357	95.2	1.314	+ 3.3
			810	147		107.2	1.360	93.3	1.306	+ 4.1
4010*	71.0	29.0	587	103	4.06	32.0	1.362	28.7	1.305	+ 4.4
			545	116		30.15	1.320	28.6	1.303	+ 1.3
			587	103	9.1	105.6	1.352	93.6	1.312	+ 3.0
4018	1.0	99.0	1001	134	4.06	22.5	1.178	22.2	1.172	+ 0.5
			999	156		22.4	1.176	22.0	1.167	+ 0.8
			1001	134	9.1	69.5	1.195	67.1	1.182	+ 1.1
			999	156		70.1	1.198	66.1	1.176	+ 1.9
4020	24.3	75.7	901	166	4.06	22.3	1.174	23.2	1.191	- 1.4
			905	228		22.76	1.184	70.6	1.201	- 1.4
			901	166	9.1	68.57	1.190	23.0	1.179	+ 0.9
			905	228		70.77	1.202	68.2	1.188	+ 1.2
4021	24.3	75.7	1031	183	4.06	22.95	1.188	23.0	1.188	0
			1033	249		22.9	1.187	23.0	1.188	- 0.1
			1031	183	9.1	70.96	1.203	67.7	1.184	+ 1.6
			1033	249		70.37	1.200	68.0	1.186	+ 1.2
4022	24.3	75.7	1115	230	4.06	22.9	1.187	22.5	1.179	+ 0.7
			1077	264		22.93	1.188	22.3	1.173	+ 1.3
			1115	230	9.1	70.26	1.199	68.3	1.189	+ 0.8
			1077	264		70.53	1.201	67.2	1.182	+ 1.6
4023			N o	D a t a						
4024	44.7	55.3	998	162	4.06	23.7	1.205	25.0	1.232	- 2.2
			989	206		25.44	1.241	23.9	1.222	+ 1.6
			998	162	9.1	75.94	1.229	78.2	1.240	- 1.1
			989	206		86.4	1.278	77.8	1.238	+ 3.2
4025	45.2	54.8	805	137	4.06	26.06	1.253	25.2	1.238	+ 1.2
			809	182		25.6	1.245	24.8	1.229	+ 1.3
			805	137	9.1	84.0	1.267	79.3	1.245	+ 1.8
			809	182		86.0	1.276	78.3	1.240	+ 2.9

*Asterisk denotes large chamber.
All remaining runs utilized the small chamber.

TABLE XIII (Con't)

TEST DATA FOR N_2/CF_4 MIXTURE USING CONICAL NOZZLE

Run 2AX	% N_2	% CF_4	P_{ch} psia	T_{ch} °F	A_e/A_t	Experimental P_c/P_e	Experimental $\overline{\gamma}$	Theoretical P_c/P_e	Theoretical $\overline{\gamma}$	% Error in Gamma
4026	45.2	54.8	748	129	4.06	25.94	1.252	25.4	1.240	+ 1.0
			621	173		26.0	1.253	24.9	1.231	+ 1.8
			748	129	9.1	87.87	1.284	79.0	1.244	+ 3.2
			621	173		87.1	1.281	77.6	1.237	+ 3.6
4027	45.5	54.5	1105	158	4.06	24.57	1.223	25.1	1.235	- 1.0
			1103	224		26.4	1.260	24.5	1.221	+ 3.2
			1105	158	9.1	77.93	1.238	79.5	1.246	- 0.6
			1103	224		87.1	1.281	77.0	1.234	+ 3.8
4028	45.5	54.5	915	169	4.06	26.07	1.253	25.0	1.232	+ 1.7
			922	232		26.2	1.257	24.4	1.220	+ 3.0
			915	169	9.1	86.8	1.279	79.0	1.244	+ 2.8
4029	65.1	34.9	1108	191	4.06	29.46	1.317	27.1	1.274	+ 3.4
			1108	191	9.1	104.04	1.349	90.0	1.293	+ 4.3
4030	65.8	34.2	903	150	4.06	29.2	1.311	27.5	1.282	+ 2.3
			839	192		29.2	1.311	27.2	1.275	+ 2.8
			903	150	9.1	101.1	1.338	89.5	1.291	+ 3.6
			839	192		101.5	1.339	89.3	1.290	+ 3.8

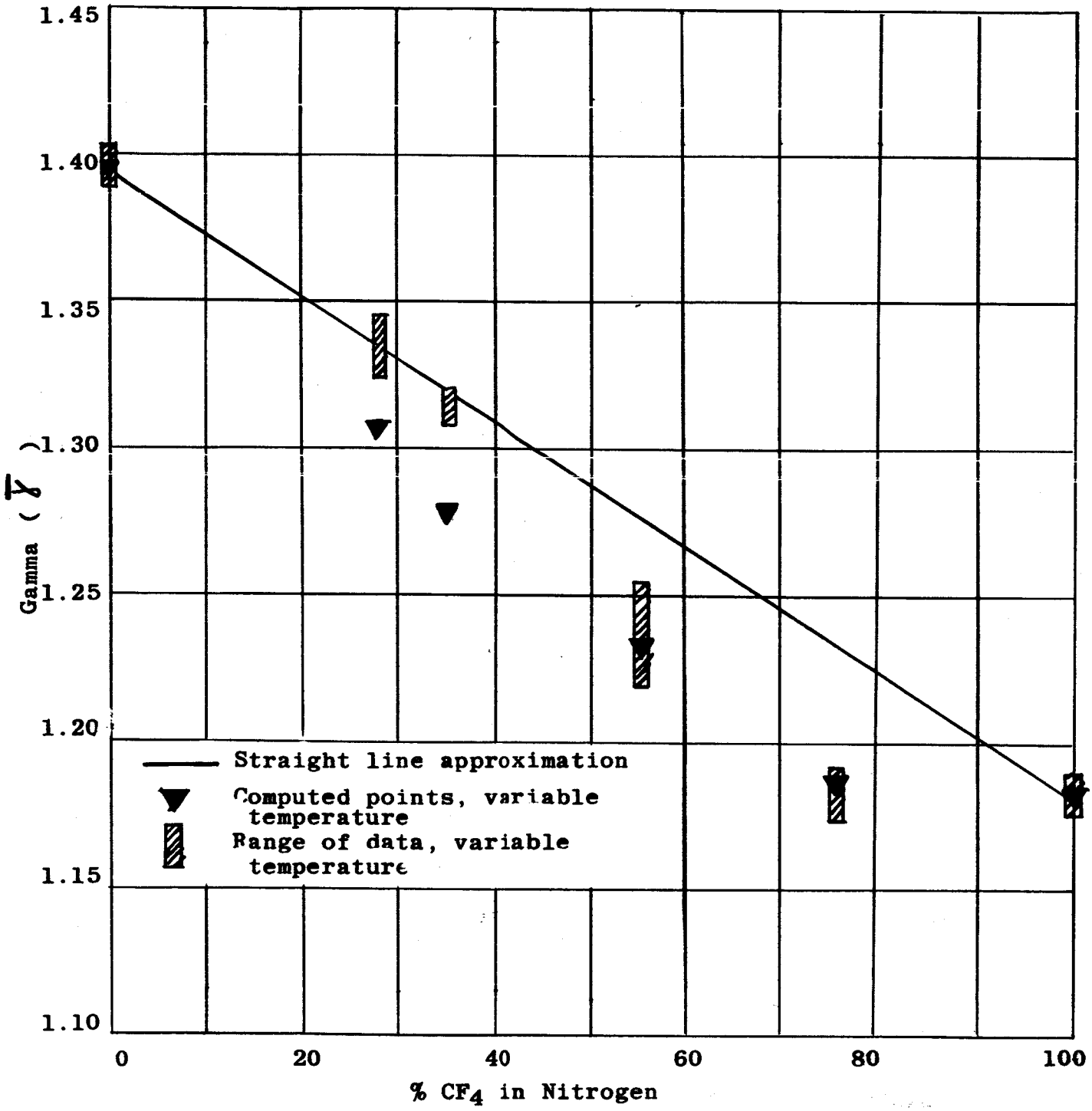

Figure 15. Gamma of CF_4/N_2 Mixtures vs. Mixture Ratio for $\epsilon = 4.06$

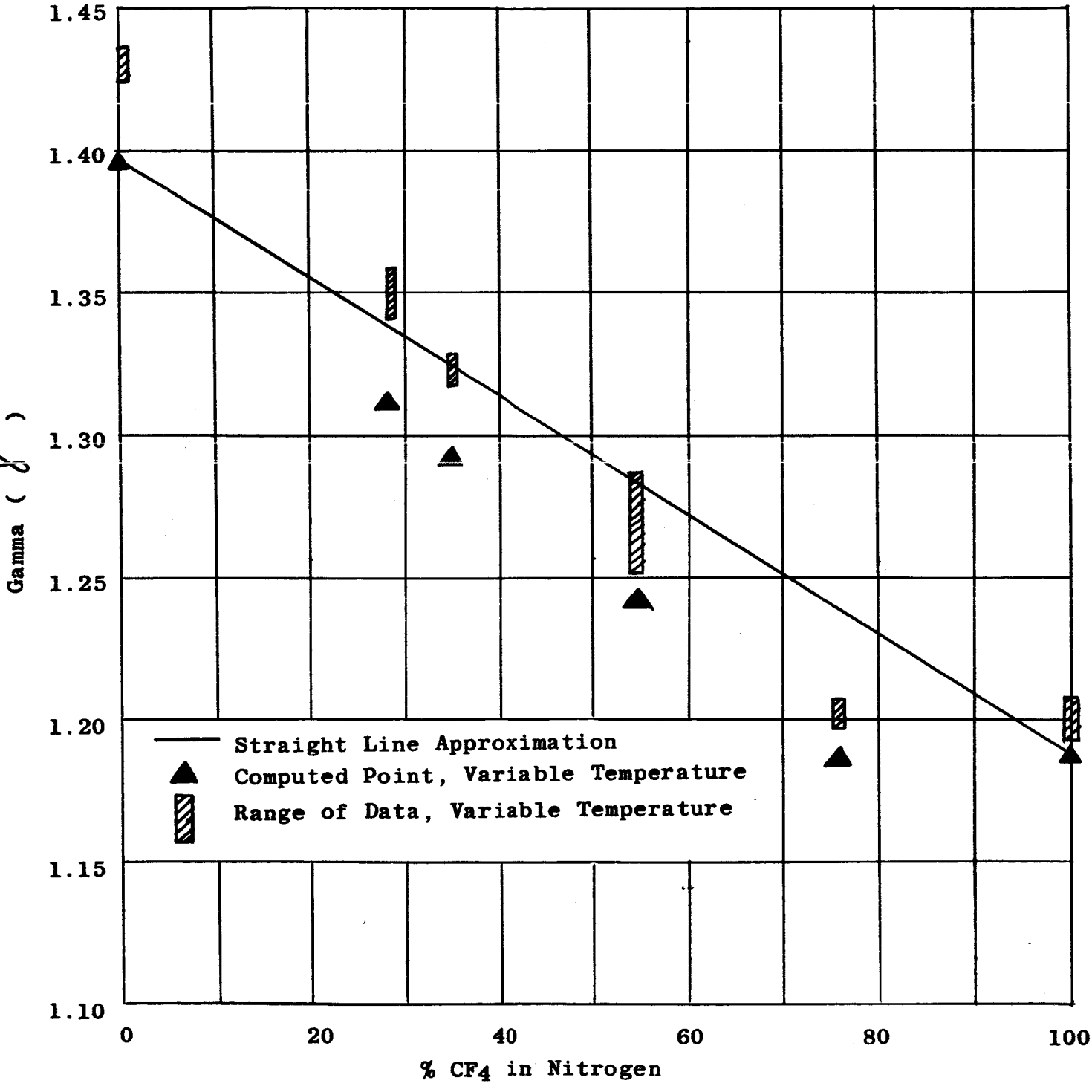

Figure 16. Gamma of CF_4/N_2 Mixtures vs. Mixture Ratio at $\epsilon = 9.1$

Table XIV shows test data for both binary and ternary mixtures containing $CHClF_2$. Since the simulant was partially liquified when loading the tank, the mixtures (computed by Dalton's mixing law) are in doubt for runs 3996 through 3999. Hence, more $CHClF_2$ was probably present than computed and the lower-than-theoretical gammas tend to verify this since the usual error was positive, and in this case it is negative. The degree of error is too small, however, to draw any definite conclusions.

Runs 4031 to 4033 used gaseous $CHClF_2$ only. Since the quantity of $CHClF_2$ is small, the data is dominated by the $N2/CF_4$ mixture behavior. The errors, however, are about the same as for the other mixtures, averaging out to +1.78% with a scatter of 4.9%.

TABLE XIV

TEST DATA ON $CHClF_2$-CONTAINING MIXTURES

Run 2AX	% N_2	% CF_4	% F22*	P_{ch} psia	T_c °F	A_e/A_t	Experimental P_c/P_e		Theoretical P_c/P_e		Chamber	% Error in Gamma
3996	62	—	38	830	76	4.06	26.7	1.266	28.5	1.300	Large	- 2.6
3997	↓		↓	570	144	4.06	26.1	1.255	27.8	1.288	Large	- 2.6
				602	190		26.7	1.266	27.4	1.281		- 1.2
3998				404	102	4.06	27.3	1.278	28.1	1.296	Large	- 1.4
				418	142		26.7	1.266	27.8	1.288		- 1.7
3999				No Data								
4031	45.0	48.1	6.9	936	152	4.06	25.04	1.233	25.2	1.237	Small	- 0.3
				928	208		26.4	1.260	24.6	1.226		+ 2.8
				936	152	9.1	77.6	1.237	80.1	1.248		- 0.9
				928	208		78.2	1.240	77.6	1.237		+ 0.2
4032				916	191	4.06	25.1	1.234	24.8	1.229		+ 0.4
				737	359		25.3	1.238	23.4	1.201		+ 3.1
				916	191	9.1	81.6	1.256	78.3	1.241		+ 1.2
				737	359		82.37	1.259	72.5	1.211		+ 4.0
4033				604	225	4.06	25.46	1.241	24.5	1.223		+ 1.5
				511	335		25.8	1.249	20.5	1.203		+ 3.8
				604	225	9.1	84.04	1.267	77.0	1.231		+ 2.9
				511	335		79.35	1.245	72.9	1.213		+ 2.6

*F-22 denotes "Freon 22", $CHClF_2$

D. Expected Errors and Observed Differences

The following expected relative error estimates have been provided by the test instrumentation group, based on past experience:

(1)	Error in reading R cal trace	1.0%
(2)	Error in reading data trace	1.0%
(3)	Teledyne pickup error	1.0%
(4)	Pressure calibration error	1.5% (Pexh)
		0.2% (Peh)
(5)	Temperature calibration error	3.3%

These estimates can be used as coefficients of variation which are well suited to estimating average expected errors on computed values. As an example, consider a computed value, $U(x,y)$, which is found by multiplication of two measured errors in the respective values. The expected errors in the measured values are taken equal to the standard deviation computed from the data: i.e., $\Delta x = \sigma x$ and $\Delta y = \sigma y$. The relative errors (coefficients of variation) are

$$\sigma x/x = \Delta x/x \; ; \quad \sigma y/y = \Delta y/y \; ; \quad \sigma U/U = \Delta U/U$$

A Taylor series expansion gives

$$\Delta U \approx y\Delta x + x\Delta y$$

which results in the variation ($\sigma^2 U$) being estimated by

$$\Delta U^2 \approx y^2\Delta x^2 + x^2\Delta y^2$$

Dividing by $(xy)^2$ we obtain

$$\Delta U^2/(xy)^2 = (\Delta x^2/x^2) + (\Delta y^2/y^2)$$

If the coefficients of variation are denoted by $V_{x,y,U}$, then V_U becomes

$$V_U = \sqrt{V_x^2 + V_y^2}$$

A similar analysis would show that if $U = x/y$ we still obtain

$$V_U = \sqrt{V_x^2 + V_y^2}$$

In reducing the nozzle flow test data, divisions and multiplications are performed in several steps on the measured values as follows:

(1) A multiplication constant K is determined in the calibration process to give K=PSIG/inch.

(a) For exhaust pressures, the coefficient of variation of the calibration pressure is estimated to be 1.5%. K is determined by measuring the R Cal with a 1% variation.

$$K = \frac{\text{Calibration Pressure}}{\text{P Cal Reading}}, \quad \text{therefore, } V_K = \sqrt{(1.5)^2 + 1.0} = 1.8\%$$

(b) Similarly for chamber pressures

$$V_K = \sqrt{(0.2)^2 + 1.0}\,\% = 1.0\%$$

(2) A data point reading is made with an expected reading error of 1.0% and then the corresponding pressure is determined by multiplying this value by K.

(a) Pch = K·(Reading) $V_{P_c} = \sqrt{V_K^2 + V_R^2} \cong 1.4\%$
(b) Pexh = K·(Reading) $V_{P_e} = \sqrt{V_K^2 + V_R^2} \cong 2.1\%$

(3) If we ignore the error introduced in converting from PSIG to PSIA (adding approximately 14.4) we get an estimated coefficient of variation for the pressure ratio of $V_{P_c/P_e} = \sqrt{V_{P_c}^2 + V_{P_e}^2} = 2.5\%$

The effect on γ of this average expected error in Pch/Pexh is shown below:

	Pc/Pe	Expected error (%)	
Ae/At=4	14.0	1.2	(γ =1.1s)
	23.0	1.1	(γ =1.2)
	27.8	1.0	(γ =1.3)
	33.6	0.9	(γ =1.4)
Ae/At=9	60.71	0.9	(γ =1.15)
	69.37	0.8	(γ =1.2)
	90.21	0.7	(γ =1.3)
	116.85	0.7	(γ =1.4)

If we use 2σ limits, a 2% relative error in the test values would not be unexpected. Visual inspection of the data shows that the "errors" are random but exist in the following apparent patterns: (The term "error" is used here for deviation from theoretical).

(1) The errors in the mixtures are, in general, greater than the errors in the "neat" cases. This is to be expected because of the uncertainty of using a straight-line approximation.

(2) In some cases, greater errors seem to be associated with the small chamber.

(3) Two measurements were made on each run. The relative error is, in general, greater for the latter of the two measurements.

(4) Greater error occurs in the higher area ratio measurements. There also seems to be a tendency for even greater error to occur when the exit pressure is below ambient pressure.

The larger errors indicated for the tests involving mixtures of gases can stem from three sources. The first possibility is that the gases do not mix according to the assumed gas law so that the use of the VanderWaal's Equations in the theoretical analysis is not adequate. The second possibility lies in the errors inherent in the mixing processes. The mixtures were not measured by weight but were determined by pressure and temperature measurements and then computed by VanderWaal's and Dalton's equations.

The third possible source of error in the mixture data may stem from use of the small chamber. A comparison of the nitrogen runs in the two chambers shows that the relative error introduced by using the small chamber is noticeably larger than the error found in tests using the large chamber.

VI. CONCLUSIONS AND RECOMMENDATIONS

A. Theoretical Conclusions and Recommended Simulants

The theoretical screening and selection process is completely adequate for selecting simulants for a known set of conditions. Gamma and Mach number can be matched simultaneously using either neat or mixed fluorocarbons depending on the actual system being simulated. The gases most useful to simulation and their qualitative extent of simulating the viscous flow parameter are summarized below. C_2F_6 is omitted at high altitudes and Mach numbers due to the possibility of condensation.

Approximate Altitude Range	Mach No.	Gas or Mixture	Viscous Flow Simulation
0-30,000 ft.	0-3.0	$CF_4/C_2F_6/N_2$	Fair
0-40,000 ft.	0-3.5	$CF_4/C_2H_2F_2/N_2$	Fair
0-30,000 ft.	0-3.0	C_2F_6/N_2	Good
0-100,000 ft.	0-5.0	CF_4	Poor

Higher altitudes may be possible with CF_4 depending on the stagnation temperature allowed in the wind-tunnel. If the wind tunnel could duplicate the actual atmospheric temperatures at altitude regardless of Mach number, the C_2F_6-containing mixtures could be used over the entire range. At exit plane pressures of approximately 6 psia, C_2F_6 will condense to a solid if the Mach number exceeds 3 with a tunnel total temperature of 700°F. If tunnel temperature can be increased, so then can the Mach number while using C_2F_6.

Neat CF_4 is useful, but at the expense of the viscous flow similitude. This is due to the higher chamber temperature required to simulate gamma.

Use of $C2H_2F_2$ in a mixture extends the Mach number slightly due to its higher vapor pressure at low temperatures. This gas, however, is questionable from a flammability standpoint. Care would have to be taken that its concentration never exceeds 5% of the total air supply in the tunnel. This is believed to be an easy requirement to meet, and it is non-toxic.

Figure 17 is a comparison of gamma values obtained with three previously used simulation methods, CF4 and a $CF_4/C_2F_6/N_2$ mixture. Note that CF_4 and the ternary mixture both come within 2% of the required value of $\overline{\gamma}$ for the F-1 engine, whereas other methods do not.

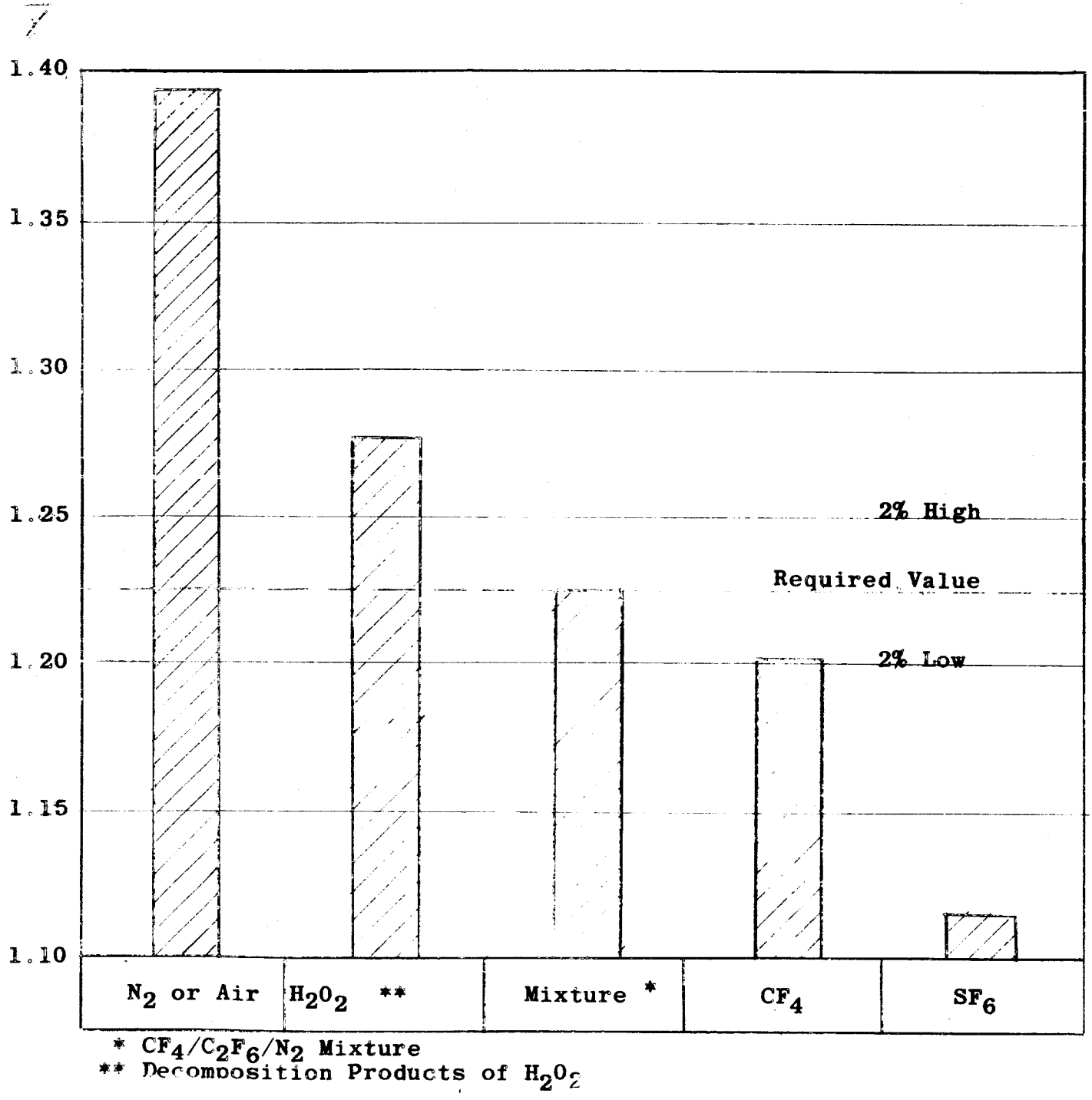

Figure 17 Typical Gamma Values of Selected Simulant Mixture* Compared with N_2, H_2O_2**, CF_4 and SF_6

B. Conclusions from the Experimental Results

Mixtures of CF_4 and N_2 have demonstrated a reasonably close agreement with theoretical results. The errors encountered were of the same general magnitude as the expected scatter (See Sect. V-D). The systematic errors were considered too small to justify changing the theoretical properties data at this time. Mixtures can, however, be changed slightly in accordance with data of the type illustrated in Figure 15. It is concluded that CF_4 has been well characterized and is ready for use in specific applications.

$CHClF_2$, which was used to gain additional experience with mixtures, is not considered a candidate. Difficulties in mixing and determining mixture ratios, along with dubious data and condensation problems combined to eliminate it from consideration. The fact is also established that no simulant in its general boiling point category may be considered.

C. Recommendations

It is recommended that a ternary mixture and neat CF_4 be considered for use in specific applications. Steps leading to this should include:

(1) A choice based on analytical work, between C_2F_6 and $C_2H_2F_2$ in the ternary mixture.

(2) Design of a test nozzle approximating the actual engine to be simulated.

(3) A study of the turbine exhaust similitude requirements, leading to the selection of a simulant for that portion of the flow.

(4) Tests with improved measurement capabilities on the ternary mixture selected, using the newly designed nozzle.

(5) Design and construction of the wind-tunnel model engine cluster according to the similitude requirements set forth in this report.

VII. BIBLIOGRAPHY

1. Adamson, T.C.; "The Structure of the Rocket Exhaust Plume Without Reaction at Various Altitudes", U. of Michigan, June, 1963.

2. Adamson, T.C., Jr. and Nicholls, J.A., "On the Structure of Jets from Highly Underexpanded Nozzles Into Still Air", Journal of the Aeronautical Sciences, January 1959, pp 16-29.

3. Barnes, L.T. and Parker, J.R.; "An Evaluation of Base Heating and Performance of a Missile Model Having Four Rocket Exhausts and a Single Base Shroud", AEDC-TN-60-63, April, 1960.

4. Bray, K.N.C., "Atomic Recombination in a Hypersonic Wind Tunnel Nozzle". J. Fluid Mechanics, Vol. 6, 1959.

5. Clarke, J.F. and McHeaney, M., "The Dynamics of Real Gases", Butterworths, Washington, 1964.

6. Englert, G.W.; "Operational Method of Determining Initial Contour and Pressure Field About a Supersonic Jet"; NASA TND-279, April, 1960.

7. Falanga, R.A., Hinson, W.F., and Crawford, D.H.; "Exploratory Tests of the Effects of Jet Plumes on the Flow Over Cone-Cylinder-Flare Bodies"; NASA TN-D-1000, Feb. 1962.

8. Goethert, B.H. and Barnes, L.T.; "Some Studies of the Flow Pattern at the Base of Missiles with Rocket Exhaust Jets" ETF, ARO, Inc., AEDC-TR-58-12; June, 1960.

9. Goethert, B.H.; "Base Flow Characteristics of Missiles with Cluster-Rocket Exhausts" Aerospace Engineering, Mar., 1961.

10. Hensel, R.W. "Transonic and Supersonic Wind-Tunnel Techniques" J. Spacecraft and Rockets, 1, (Sept.-Oct. 1964).

11. Henson, J.R. and Robertson, J.E.; "Methods of Approximating Inviscid Jet Boundaries for Highly Under-expanded Supersonic Nozzles", ARO, Inc., AEDC-TDR-62-7, May, 1962.

BIBLIOGRAPHY (Cont'd)

12. Korst, H.H., Chow, W.L., and Zumwalt, G.W., "Research on Transonic and Supersonic Flow of a Real Fluid at Abrupt Increase in Cross Section," ME Technical Report 329-5, University of Illinois.

13. Korst, H.H., "A Thoery of Base Pressure in Transonic and Supersonic Flow", J. of Applied Mechanics, Vol. 23, 1956, pp. 593-600.

14. Korst, H.H., Page R.H. and Childs, M.E., "A Theory for Base Pressure in Transonic and Supersonic Flow", University of Illinois, ME-TN-392-2, 1955.

15. Korst, H.H., and Tripp, W., "The Pressure on a Blunt Trailing Edge Separating Two Supersonic Two-Dimensional Air Streams of Different Mach Number and Stagnation Temperature", Proc. of the Fifth Midwestern Conference on Fluid Mechanics, University of Michigan, April 1957, pp 187-199.

16. Latvala, E.K.; "Spreading of Rocket Exhaust Jets at High Altitudes"; ETF, ARO, Inc.: AEDC-TR-59-11, June 1959.

17. Liepmann, H.W., and Roshko, A., "Elements of Gas Dynamics", J. Wiley and Son, Inc., New York, 1958.

18. Literature on Gas Properties from Matheson Co.

19. Lieterature on Gas Properties from Air Products and Chemicals, Inc.

20. Love, E.S.; Grigsby, C.E.; Lee, L.P.; and Woodling, M.J.; "Experimental and Theoretical Studies of Asisymmetric Free Jets"; NASA TR R-6; 1959.

21. "Properties of Commonly Used Refrigerants"; 1957, ed. Air-Conditioning and Refrigeration Institute.

22. RMD Monthly Reports; Project 5804, "Gas Mixtures for Dynamic Simulation of Rocket Exhaust Jets". Reports M1 through M7.

23. Symposium Proceedings; "Simulated Altitude Testing of Rockets and Missile Components", Dec. 1-2, 1959; AEDC-TR-60-6, March 1960.

24. Schlumpf, R.L. and Clark, H.K.; "Spreading of Hydrogen-Air Rocket Exhaust Jets at High Altitudes"; ETF, ARO, Inc.; AEDC-TN-59-131, Nov. 1959.

APPENDIX A

PROGRAM NO. D1198, "CHARACTERIZATION OF SIMULANT FLUIDS"

FLOW CHART

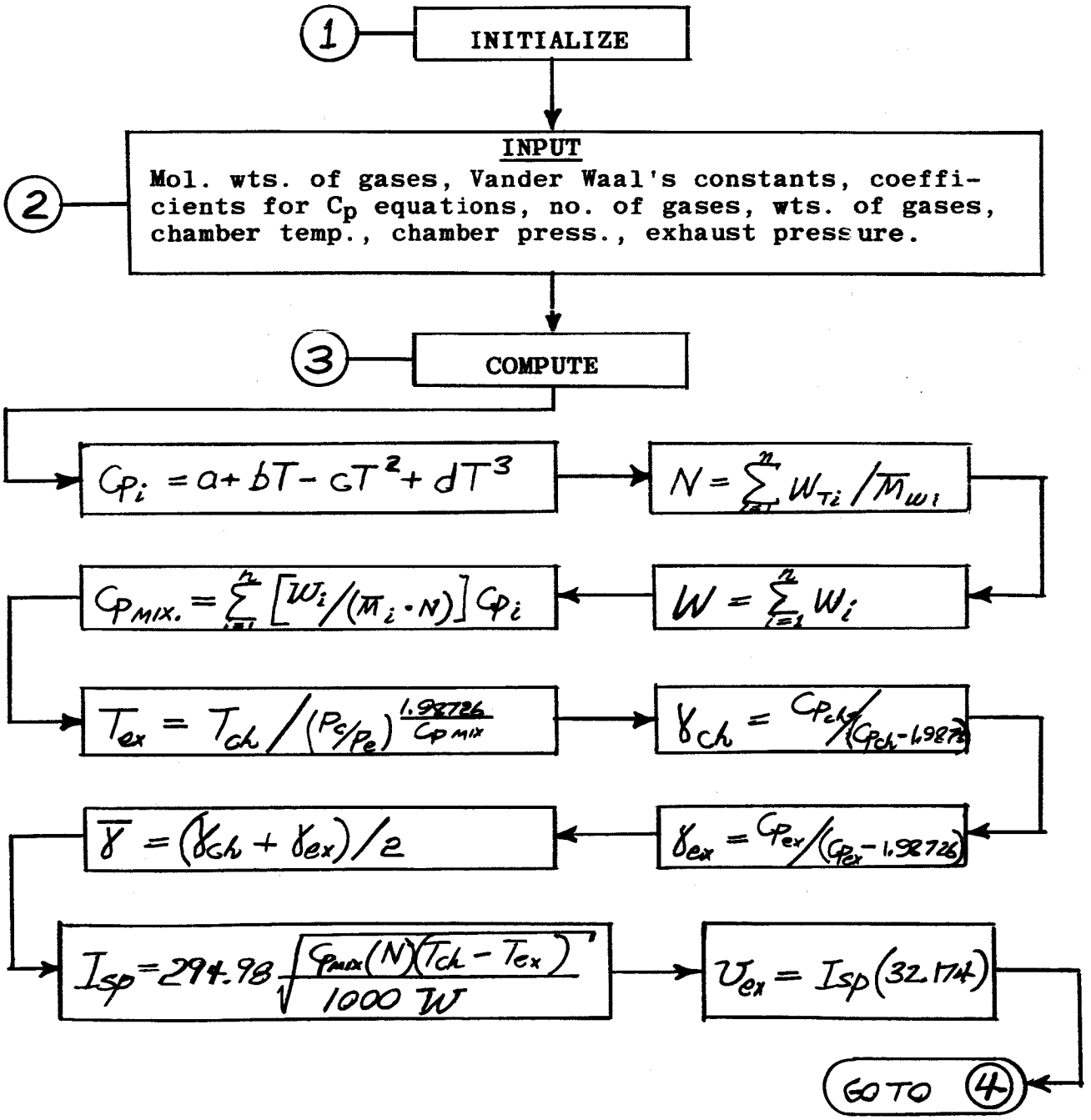

PROGRAM NO. D1198
(Con't)

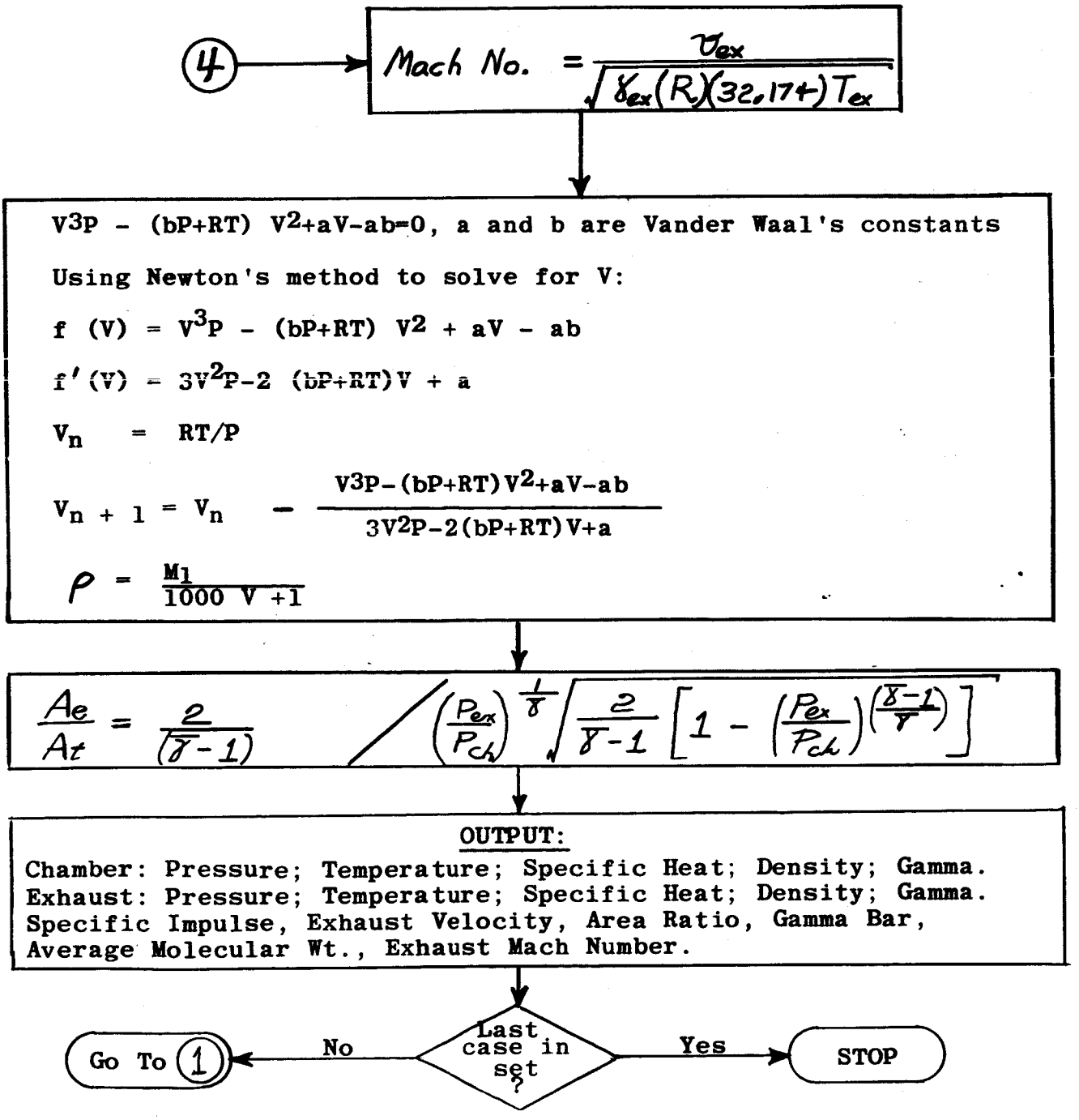

APPENDIX A (Con't)

EQUATIONS FOR PROGRAM D1198

$$C_{p_{mixture_{ch}}} = \frac{\gamma_1}{M_{1n}} C_{p_{1ch}} + \frac{\gamma_2}{M_{2n}} C_{p_{2_{ch}}} + \cdots\cdots \frac{\gamma_n}{M_{nn}} C_{p_{n_{ch}}} \qquad (1)$$

$$T_{ex} = \frac{T_c}{\frac{P_c}{P_e}\left(\frac{1.987}{C_{p_{mixture_{ch}}}}\right)} \quad \text{(degrees Kelvin)} \qquad (2)$$

$$\gamma_{ch} = \frac{C_{p_{mixture_{ch}}}}{\left(C_{p_{mixture_{ch}}} - 1.987\right)} \qquad (3)$$

$$I_{sp} = 294.98 \sqrt{\frac{C_{p_{mixture}} \cdot n \cdot (T_c - T_e)}{1000.w}} \qquad (4)$$

w = total weight of ingredients

$$\gamma_{ex.} = \frac{C_p \text{ mixture ex.}}{\left(C_p \text{ mixture ex.} - 1.987\right)} \qquad (5)$$

$v_{exh.}$ = velocity at exhaust = Isp x 32.174

$$\text{Mach No. exh.} = \frac{v_{exh.}}{\sqrt{\gamma_{exh.} \cdot R \cdot 32.174 \cdot T_e}} \quad \left(\text{where } T_e \text{ is in } {}^{o}R \text{, } R = 64.4\right) \qquad (6)$$

$$v^3 p - (bP + RT)\, v^2 + aV - ab = 0 \quad \left(\text{where a and b are Vander Waal's constants}\right) \qquad (7)$$

APPENDIX A (Con't)

Using Newton's convergence to solve the above equation for V

$$f(V) = V^3P - (bP + RT)\,V^2 + aV - ab \tag{8}$$

$$f(V) = 3V^2P - 2(bP + RT)\,V + a \tag{9}$$

$$V_n = \frac{RT}{P} \tag{10}$$

$$V_{n+1} = V_n - \left(\frac{V^3P - (bP + RT)\,V^2 + aV - ab}{3V^2P - 2(bP + RT)\,V + a}\right) \tag{11}$$

$$\rho = \frac{M_1}{1000\,V_n + 1} \tag{12}$$

$$\bar{\gamma} = \frac{\gamma_{CH} + \gamma_{exh}}{2} \tag{13}$$

$$\epsilon = \frac{\left[\frac{2}{(\bar{\gamma}+1)}\right]^{\frac{\bar{\gamma}+1}{2(\bar{\gamma}-1)}}}{(P_e/P_c)^{1/\bar{\gamma}}\sqrt{\frac{2}{\bar{\gamma}-1}\left[1-(P_e/P_c)^{\frac{\bar{\gamma}-1}{\bar{\gamma}}}\right]}} \tag{14}$$

```
      PROGRAM NO.D1198,SIMULANT FLUID CHARACTERIZATION.    M
      200 ABCONS
      53 IS HIGHEST STATEMENT NUMBER
      DIMENSION X(30) Y(60) C(70)          G(60)  Z(40) N
           H(20) I(5) J(5)   D(80)
      X21 IS THE CHAMBER PRESSURE. X22 IS THE EXHAUST      M
      PRSSURE. X20 AND X23 IS THE CHAMBER TEMPERATURE      M
      OUTPUT                                               M
      X24,X25 ARE THE EXHAUST TEMPERATURE. Y1 IS GAMMA.    M
      Y2 IS ISP. Y10 IS CP BAR IN  THE CHAMBER.            M
      Y4 IS THE CHANGE OF HEAT CONTENT BETWEEN CHAMBER     M
      AND EXHAUST.  Y11 IS CP BAR AT EXHAUST.  Y7 IS       M
      GAMMA AT EXHAUST.  Y8 IS VELOCITY AT EXHAUST.        M
      Y9 IS MACH NUMBER AT EXHAUST.                        M
      Z1....Z11 ARE DENSITIES                              M
      Z21...Z31 ARE DENSITIES. Y14 IS AREA RATIO           M
    1 READ
      X23←273.15+(X20-32.0)/1.8
      X12←0; Y5←0; Y11←0; Z14←0; Z18←0; Y3←0
       10,J2,1,1,J1,
       X12←X12+X(J2)
       Y5←Y5+XJ2/GJ2
      Z13←D(4*J2-4)+D(4*J2-3)*X23+D(4*J2-2)*X23↑2  N
         +D(4*J2-1)*X23↑3
   10  Y3←Y3+Z13*XJ2/GJ2
       Y10←Y3/Y5
      G12←X12/Y5
      X24←X23/(X21/X22)↑(1.987/Y10)
      X25←((X24-273.15)*1.8)+32.0
      Y1←Y10/(Y10-1.987)
      Y4←Y10*Y5*(X23-X24)/1000.
      Y2←(294.98)*SQRT.(Y4/X12)
       20,J2,1,1,J1,
      Z17←D(4*J2-4)+D(4*J2-3)*X24+D(4*J2-2)*X24↑2  N
         +D(4*J2-1)*X24↑3
   20  Y11←Y11+Z17*XJ2/(GJ2*Y5)
      Y7←Y11/(Y11-1.987)
      Y8←(Y2)*32.174
      Y9←Y8/SQRT.(Y7*1545*32.174*1.8*X24/G12)
      <2(E)>
      TX1...XJ1
      TG1...GJ1
       50,J2,1,1,J1,
       H0←.082*X23*14.7/X21
       I1←-1
       GO TO 31 IF CJ2=0
       Y21←CJ2*X21/14.7+.082*X23
       Y22←CJ2*C(J2+20)
       Y23←CJ2*X22/14.7+.082*X24
       30,I1,0,1,7,
      H(I1+1)←HI1  -((((HI1↑3)*X21/14.7)-Y21*(HI1↑2)+ N
       C(J2+20)      *HI1-Y22)/((3*(HI1↑2)*X21/14.7)  N
           -2*Y21*HI1+C(J2+20)))
   30 GO TO 31IF H(I1+1)-HI1<0.001
   31  ZJ2     ←GJ2     /(1000.*H(I1+1))
       H0←.082*X24*14.7/X22
       I1←-1
       GO TO 41 IF CJ2=0
       40,I1,0,1,7,
      H(I1+1)←HI1-((((HI1↑3)*X22/14.7)-Y23*(HI1↑2)+ N
```

```
      C(J2+20)      *HI1-Y22)/((3*(HI1+2)*X22/14.7)  N
          -2*Y23*HI1+C(J2+20)))
40    GO TO 41IF H(I1+1)-HI1<0.001
41     Z(J2+20)+GJ2      /(1000.*H(I1+1))
       Z14+Z14+XJ2/ ZJ2
       Z18+Z18+XJ2/Z(J2+20)
50     Z15+X12/Z14
       Z16+X12/Z18
      Y12+(Y1+Y7)/2
      Y13+(2/(Y12+1))+((Y12+1)/(2*(Y12-1)))
      Y14+((X22/X21)+(1/Y12))*SQRT.((2/(Y12-1))*(1- N
      ((X22/X21)+((Y12-1)/Y12))))
      Y15+Y13/Y14
      <R25,  $ AT  CHAMBER $,E>
      PTX21TX22
      <R10,$ PCH. = $, 4D.3Z,12S, $ P EX.  = $,4D.3Z,E>
      PTX20TX25
      <R10,$ TCH   = $,4D.3Z,13S,$TEX. = $,-4D.2Z,E>
      PTY10TY1
      <R10,$ CP BAR = $,4D.3Z, 9S,$ GAMMA      = $,2D.  N
      3Z,E>
      PTY2
      <R10,$ ISP   = $,4D.2Z,E>
      PTZ15
      <R10,$ DENSITY CH. = $, 2D.4Z,E>
      <R25,$ AT EXHAUST $, E>
      PTY11TY7
      <R10,$ CP EXH. = $,4D.3Z,8S, $ GAMMA      = $,2D.  N
      3Z,E>
      PTY8
      <R10,$ VELOCITY = $, 6D.3Z,E>
      PTY9
      <R10,$ MACH NO. EXH. = $,3D.2Z,E>
      PTZ16
      <R10,$ DENSITY EXH. = $, 2D.4Z,E>
      <2(E)>
      PTY12
      <R10, $  GAMMA BAR   = $, 2D.3Z,E>
      PTY15
      <R10, $  AE/AT  =  $,  3D.2Z,E>
      PTG12
      <R10,$ AVE.MOL.WT. = $, 3D.3Z,E>
      <2(E)>
      GO TO 1
      HALT
      PROGRAM END
                          00:00:28
```

APPENDIX B

THERMODYNAMIC DATA AND SIMULANT PERFORMANCE

The following pages contain the equations and known thermodynamic data which have been used in simulant characterization and screening. The final series of tables (unnumbered) illustrate the performance parameters obtained with several simulants. Since CF_4 has been found to be the most applicable simulant ingredient there is an appropriately larger amount of performance data on CF_4. Theoretical graphs and tables appearing earlier in this report are based on these data.

Most of the data shown below have been supplied by the DuPont Company's Freon Products Division. Other sources were: The Matheson Co.; Air Products, Inc., Union Carbide, The JANAF Thermochemical Tables, NBS Bulletins, Refs. 5 and 21, and empirical estimates made at Thiokol-RMD.

In the following table of force constants and viscosities, σ = the low velocity collision diameter in angstrom units, ϵ/K is the intermolecular force constant and μ is the viscosity in micropoise.

FORCE CONSTANTS AND VISCOSITI

COMPOUND	σ	ϵ/K	100	200	300
Ar	3.542	93.3	87.7	166.0	229.0
$CBrF_3$	5.01	235.	53.5	106.5	159.4
$CClF_3$	4.96	188.	50.6	101.9	150.2
CCl_2F_2	5.25	253.	42.5	84.1	126.3
CF_4	4.662	134.	62.4	123.9	176.7
$CHClF_2$	4.68	261.	44.7	88.1	132.4
CHF_3	4.33	240.	48.7	96.7	144.8
CH_2ClF	4.48	318.	40.3	77.2	116.6
CH_2F_2	4.08	318.	42.3	81.1	122.5
CH_3Cl	4.182	350.	38.3	72.5	109.4
CH_3F	3.73	333.	40.3	76.7	115.8
CO_2	3.941	195.2	51.1	102.8	152.
N_2	3.798	71.4	72.4	131.3	177.7
N_2O	3.828	232.4	50.	99.7	149.2
SF_6	5.128	222.1	51.8	103.6	154.6

TABLE XV

ES FOR CANDIDATE SIMULANT GASES

Viscosity, μ at temperatures (^{o}K)						
400	500	600	700	800	900	1000
282.9	330.6	374.4	415.3	453.8	490.1	524.7
208.3	252.7	293.3	330.9	366.2	399.4	431.
193.1	231.5	266.6	299.1	329.4	358.	385.1
165.9	202.1	235.3	266.1	294.9	322.2	347.9
222.2	262.7	299.6	333.6	365.5	395.9	425.
174.3	212.7	247.9	280.6	311.3	340.3	367.7
189.6	230.3	267.5	302.	334.4	364.4	393.9
155.	191.3	225.	256.4	285.9	313.8	340.3
162.9	201.	236.5	269.5	300.5	329.8	357.6
145.9	180.9	213.8	244.5	273.4	300.8	326.8
154.2	190.8	224.9	256.8	286.7	315.	341.9
196.	235.4	271.4	304.8	335.9	365.3	393.1
217.2	252.7	285.4	315.6	344.	371.	397.1
94.8	236.2	274.	309.1	342.	372.	402.4
01.3	243.3	281.8	317.5	350.9	382.4	412.3

P. 75 (2)

APPENDIX B (Con't)

TABLE XVI

VAN DER WAAL'S CONSTANTS FOR SIMULANT FLUIDS:

$$V^3P - (bP+RT)V^2+aV-ab = 0$$

FLUID	a	b
$CClF_3$	0.081	6.769
SF_6	0.0881	7.771
CF_4	0.0632	3.98
N_2	0.0386	1.346
CHF_3	0.06425	5.3178
CH_3Cl	0.0648	7.469
CO_2	0.0428	3.6
$CHClF_2$	0.0777	7.936
N_2O	0.04415	3.782
$CBrF_3$	0.08918	8.3966
C_2F_6	0.1021	8.2749
$C_2H_2F_2$	0.071131	5.9698

APPENDIX B (Con't)

TABLE XVII

EQUATIONS DESCRIBING SIMULANT SPECIFIC HEATS

(1) CCl_2F_2

$C_p = 3.472 + 6.801 \times 10^{-2} T - 8.412 \times 10^{-5} T^2 + 3.872 \times 10^{-8} T^3$

(2) SF_6

$C_p = -0.8929 + 1.107 \times 10^{-1} T - 1.118 \times 10^{-4} T^2 + 3.46 \times 10^{-8} T^3$

(3) CF_4

$C_p = 4.624 + 3.686 \times 10^{-2} T - 8.027 \times 10^{-6} T^2 - 1.386 \times 10^{-8} T^3$

(4) N_2

$C_p = 7.232 - 1.935 \times 10^{-3} T + 3.768 \times 10^{-6} T^2 - 1.086 \times 10^{-9} T^3$

(5) CH_2F_2

$C_p = 8.089 - 6.700 \times 10^{-3} T + 6.106 \times 10^{-5} T^2 - 4.743 \times 10^{-8} T^3$

(6) CH_3Cl

$C_p = 8.2799 - 9.378 \times 10^{-3} T + 6.168 \times 10^{-5} T^2 - 4.684 \times 10^{-8} T^3$

(7) CO_2

$C_p = 5.125 + 15.224 \times 10^{-3} T - 9.681 \times 10^{-6} T^2 + 2.313 \times 10^{9} T^3$

(8) $CHClF_2$

$C_p = 5.780 + 2.631 \times 10^{-2} T + 9.043 \times 10^{-7} T^2 - 1.369 \times 10^{-8} T^3$

(9) $CClF_3$

$C_p = 3.810 + 0.05429 T - 4.99 \times 10^{-5} T^2 + 1.493 \times 10^{-8} T^3$

(10) CHF_3

$C_p = 6.554 + 1.180 \times 10^{-2} T + 3.443 \times 10^{-5} T^2 - 3.609 \times 10^{-8} T^3$

(11) CH_2ClF

$C_p = 7.394 + 3.947 \times 10^{-3} T + 4.096 \times 10^{-5} T^2 - 3.638 \times 10^{-8} T^3$

(12) N_2O

$C_p = 6.529 + 10.515 \times 10^{-3} T - 3.571 \times 10^{-6} T^2$

APPENDIX B (Con't)

TABLE XVII, (Con't)

EQUATIONS DESCRIBING SIMULANT SPECIFIC HEATS

(13) $CBrF_3$

$$C_p = 2.097 + 2.916 \times 10^{-2}\ T - 3.151 \times 10^{-5}\ T^2 + 1.263 \times 10^{-8}\ T^3$$

(14) C_2F_6

$$C_p = 9.29 + 6.024 \times 10^{-2}\ T - 2.396 \times 10^{-5}\ T^2$$

(15) $C_2H_2F_2$

$$C_p = 8.464 + 2.849 \times 10^{-2}\ T - 1.04 \times 10^{-5}\ T^2$$

(16) C_2ClF_5

$$C_p = 3.559 + 5.508 \times 10^{-2}\ T - 2.204 \times 10^{-5}\ T^2$$

APPENDIX B (Con't)

GAS - CF_4

BOILING POINT - 198.4 °F

T_{ch} °F	850	700	550	400	212	77
P_c/P_e	1000/14.696 = 68.05					
γ_e	1.115	1.124	1.137	1.156	1.192	1.233
M_e	3.04	3.03	3.03	3.03	3.04	3.04
P_c/P_e	1000/6.70 = 149.25					
γ_e	1.120	1.130	1.144	1.164	1.204	1.250
M_e	3.37	3.36	3.36	3.37	3.38	3.39
P_c/P_e	1000/2.14 = 467.29					
γ_e	1.127	1.139	1.155	1.178	1.224	1.275
M_e	3.83	3.82	3.82	3.83	3.86	3.89
P_c/P_e	1000/1.33 = 758.87					
γ_e	1.131	1.143	1.160	1.185	1.232	1.286
M_e	4.01	4.00	4.01	4.02	4.05	4.09
P_c/P_e	1000/0.50 = 2000					
γ_e	1.139	1.152	1.171	1.198	1.251	1.310
M_e	4.39	4.38	4.39	4.41	4.46	4.52

COST: $5.00/lb.

APPENDIX B (con't)

GAS - CF_4

Boiling Point - 198.4°F.

P_{ch}, psia	1000			650			1000			1500		
T_{ch}, F	700	550	400	700	550	400	80			115		
P_{ex}, psia	14.7			14.7			6.667	5.714	5.000	8.571	7.500	6.667
T_{ex},F	323.1	208.7	91.77	355.1	237.4	117.3						
C_p CH	21.33	20.33	18.89	21.33	20.33	18.89						
γ CH	1.103	1.108	1.118	1.103	1.108	1.118						
C_p Ex	618.0	16.49	14.76	18.37	16.89	15.16						
γ Ex	1.124	1.137	1.156	1.121	1.133	1.151						
Density	.0025	.0029	.0035	.0024	.0028	.0034						
Viscosity	244	217	189	252	226	196						
Velocity	2138	1986	1819	2045	1901	1742						
$\rho v/\mu$	.0219	.0265	.0337	.0195	.0235	.0302	.0519	.0468	.0429	.0624	.0574	.0517
Mach No.	3.03 →			2.85 →			3.39	3.46	3.52	3.46	3.51	3.56
I_{sp}	66.46	61.73	56.55	63.57	59.07	54.15						
$\overline{\gamma}$	1.113	1.123	1.137	1.112	1.121	1.134	1.203	1.205	1.206	1.195	1.196	1.197
A_e/A_t	10.67	10.45	10.13	7.59	7.46	7.26						
$\overline{M}$	88.01			88.01			88.01			88.01		

Cost: $5.00/lb.

APPENDIX B (con't)

GAS - C_2F_6

Boiling Point - 108.8°F.

P_{ch} Psia	1000	→	→	650	→	→	1000	→	→	1500	→	→
Tch °F.	700	550	400	700	550	400	80	→	→	115	→	→
Pex, Psia	14.7	→	→	14.7	→	→	6.667	5.714	5.000	8.571	7.500	6.667
P_c/P_e	68.05	→	→	44.23	→	→	150	175	200	175	200	225
Tex, °F.	471.2	337.08	205.0	492.3	357.2	222.7	-100	-102	-104	-79	-81	-83
Density Ch	.1864	.2213	.2734	.1198	.1410	.1722						
Cp Ex	34.04	31.231	28.27	34.45	31.69	28.68						
γ Ex	1.062	1.068	1.076	1.061	1.067	1.074						
Density Ex	.0033	.0038	.0046	.0032	.0037	.0045						
Viscosity Ex	215	190	162	220	195	165						
Velocity Ex	1779.	1654.	1518.	1695.	1576.	1448.						
Mach No.	2.98	2.99	2.99	2.81	2.81	2.82	3.33	3.39	3.44	3.39	3.44	3.48
$\rho v/\mu$	.0273	.0331	.0431	.0246	.0299	.0395	.0404	.0359	.0322	.0483	.0439	.0392
Isp	55.30	51.40	47.18	52.68	48.99	44.99						
$\bar{\gamma}$	1.058	1.064	1.070	1.058	1.063	1.070	1.097	1.097	1.097	1.093	1.093	1.094
Ae/At	12.17	12.02	11.82	8.51	8.41	8.29						
$\bar{M}$	138.02	→	→	138.02	→	→	138.02	→	→	138.02	→	→

Cost: $2.50/lb.

APPENDIX B (Con't)

GAS - CHF_3

BOILING POINT - 115.7°F

P_{ch}, psia	1000	→		650	→	
T_{ch}, F	700	550	400	700	550	400
Pex, psia	14.696	→		14.696	→	
Tex, F	282.60	167.91	51.15	317.19	199.12	79.03
C_p CH	18.796	17.636	16.111	18.796	17.636	16.111
γ CH	1.118	1.127	1.141	1.118	1.127	1.141
Density CH	.0902	.1036	.1216	.0586	.0673	.0791
Viscosity Ch	290	260	230			
Cp Ex	14.744	13.324	11.851	15.159	13.715	12.202
γ Ex	1.156	1.175	1.201	1.151	1.169	1.195
Density Ex	.0021	.0024	.0030	.0020	.0023	.0029
Viscosity Ex	200	175	145	210	180	150
Velocity Ex	2367.9	2194.5	2004.2	2267.7	2102.9	1922.4
Mach No.	3.04	3.04	3.04	2.85	2.84	2.84
Isp	73.60	68.21	62.29	70.48	65.36	59.75
$\overline{\gamma}$	1.137	1.151	1.171	1.135	1.148	1.168
A_e/A_t	10.12	9.81	9.41	7.26	7.07	6.82
$\overline{M}$	70.019	→		70.019	→	

Cost: $5.00/lb

APPENDIX B (Con't)

GAS - CH_2F_2

BOILING POINT - 60.9°F

P_{ch}, psia	1000 →			650 →		
T_{ch}, F	700	550	400	700	550	400
P_{ex}, psia	14.696 →			14.696 →		
T_{ex}, F	236.48	121.25	5.38	273.70	154.97	35.48
C_p CH	14.433	15.172	13.650	16.433	15.172	13.650
γ CH	1.138	1.151	1.170	1.138	1.151	1.170
Density CH	.0670	.0769	.0904	.0435	.0500	.0587
Viscosity	255	230	200			
C_p Ex	11.887	10.692	9.616	12.287	11.032	9.9879
γ Ex	1.201	1.228	1.260	1.193	1.220	1.252
Density Ex	.0016	.0020	.0025	.0016	.0019	.0023
Viscosity Ex	165	140	110	170	145	120
Velocity Ex	2706.7	2501.3	2276.1	2595.8	2400.9	2187.6
I_{sp}	84.13	77.74	70.74	80.68	74.62	67.99
$\overline{\gamma}$	1.169	1.189	1.215	1.165	1.185	1.211
A_e/A_t	9.45	9.06	8.61	6.85	6.61	6.31
$\overline{M}$	52.027 →			52.027 →		

Cost: $10.00/lb

APPENDIX B (Con't)

GAS - $CClF_3$

BOILING POINT - 114.6°F

P_{ch}, psia	1000 →			650 →		
T_{ch}, F	700	550	400	700	550	400
Pex, psia	14.696 →			14.696 →		
T_{ex}, F	333.36	220.09	105.36	364.72	248.11	130.09
C_p CH	22.067	21.197	19.983	22.067	21.197	15.983
γ CH	1.099	1.103	1.110	1.099	1.103	1.110
Density Ch	.1409	.1667	.2051	.0904	.1061	.1289
Viscosity Ch	285	260	230			
C_p E_x	19.320	18.005	16.397	19.642	18.350	16.766
γ E_x	1.115	1.124	1.138	1.113	1.121	1.134
Density Ex.	.0029	.0034	.0041	.0028	.0033	.0039
Viscosity Ex	215	190	165	220	200	160
Velocity Ex	1968.6	1830.2	1679.4	1882.5	1750.8	1607.3
Mach No.	3.03	3.03	3.03	2.86	2.86	2.86
I_{sp}	61.19	56.88	52.20	58.51	54.42	49.96
$\overline{\gamma}$	1.107	1.114	1.124	1.106	1.112	1.122
Ae/At	10.83	10.66	10.41	7.79	7.58	7.43
$\overline{M}$	104.47 →			104.47 →		

Cost: $4.50/lb

APPENDIX B (Con't)

GAS-CCl_2F_2

BOILING POINT - 21.6°F

P_{ch}, psia	1000 →			650 →		
Tch, F	700	550	400	700	550	400
Pex, psia	14.696 →			14.696 →		
Tex, F	342.15	229.82	116.78	372.93	257.20	140.78
C_p CH	22.727	21.987	20.984	22.727	21.987	20.984
γ CH	1.096	1.099	1.105	1.096	1.099	1.105
Density Ch	.1721	.2067	.2591	.1087	.1291	.1595
Viscosity Ch	254	227	203			
Cp Ex	20.498	19.357	17.897	20.764	19.661	18.236
γ Ex	1.107	1.114	1.125	1.106	1.112	1.122
Density Ex	.0033	.0039	.0047	.0032	.0037	.0045
Viscosity Ex	185	165	140	195	172	147
Velocity Ex	1834.5	1706.8	1568.2	1753.9	1632.2	1500.3
Mach No.	3.03	3.03	3.03			
Isp	57.02	53.05	48.74	54.51	50.73	46.63
$\overline{\gamma}$	1.102	1.107	1.115	1.101	1.106	1.113
Ae/At	10.96	10.83	10.64	7.76	7.68	7.57
$\overline{M}$	120.925 →			120.925 →		

Cost: $0.29/lb

APPENDIX B (Con't)

GAS - $CHCLF_2$

BOILING POINT - 41.4°F

Pch, psia	1000 →			650 →		
Tch, F	700	550	400	700	550	400
P_{ex}, psia	14.696 →			14.696 →		
T_{ex}, F	293.74	180.52	66.16	327.65	210.99	93.22
Cp CH	19.445	18.406	17.060	19.445	18.406	17.060
γ CH	1.114	1.121	1.132	1.114	1.121	1.132
Density Ch	.1203	.1434	.1781	.0764	.0901	.1103
Viscosity Ch	260	240	210			
Cp Ex	15.947	14.636	13.202	16.315	15.000	13.550
γ Ex	1.142	1.157	1.177	1.139	1.153	1.172
Density Ex	.0024	.0031	.0036	.0024	.0030	.0038
Viscosity Ex	190	165	135	195	170	150
Velocity Ex	2138.1	1983.8	1815.4	2046.9	1500.2	1740.3
Mach No.	3.04	3.04	3.04	2.85	2.85	2.85
Isp	66.45	61.66	56.42	63.62	59.06	54.09
$\bar{\gamma}$	1.128	1.139	1.154	1.126	1.137	1.152
A_e/A_t	10.32	10.07	9.74	7.38	7.23	7.02
$\bar{M}$	86.476 →			86.476 →		

Cost: $0.97/lb

APPENDIX B (Con't)

GAS - CH_3Cl

BOILING POINT - 11.6°F

P_{ch}, psia	1000	→		650	→	
T_{ch}, F	700	550	400	700	550	400
P_{ex}, psia	14.696	→		14.696	→	
Tex, F	210.99	98.75	-13.95	249.55	133.55	16.96
C_p CH	15.314	14.160	12.767	15.314	14.160	12.767
γ CH	1.149	1.163	1.184	1.149	1.163	1.184
Density Ch	.0708	.0844	.1049	.0048	.0528	.0647
Viscosity Ch	230	200	178			
Cp Ex	10.926	9.908	9.029	11.295	10.212	9.252
γ Ex	1.222	1.251	1.282	1.213	1.242	1.274
Density Ex	.0017	.0020	.0025	.0016	.0019	.0024
Viscosity Ex	143			149	133	
Velcoity Ex	2724.3	2516.4	2288.6	2614.7	2417.5	2201.5
Isp	84.67	78.21	71.13	81.27	75.14	68.43
$\overline{\gamma}$	1.186	1.207	1.233	1.181	1.202	1.229
A_e/A_t	9.13	8.75	8.32	6.65	6.41	6.13
$\overline{M}$	50.497	→		50.492	50.492	50.492

Cost $0.50/lb

APPENDIX B (Con't)

GAS - SF_6

BOILING POINT - 82.0°F

P_{ch}, psia	1000	→		650	→	
T_{ch}, F	700	550	400	700	550	400
P_{ex}, psia	14.696	→		14.696	→	
T_{ex}, F	465.13	318.06	191.82	465.13	339.06	210.53
C_p CH	33.274	32.132	30.245	33.274	32.132	30.245
γ CH	1.064	1.066	1.070	1.064	1.066	1.070
Density Ch	.1994	.2369	.2929	.1275	.1501	.1832
Viscosity Ch	301	270	244			
Cp Ex	30.850	28.857	26.169	31.163	29.238	26.611
γ Ex	1.069	1.074	1.082	1.068	1.073	1.081
Density Ex	.0036	.0041	.0049	.0035	.0040	.0048
Viscosity Ex	258	223	193	258	229	197
Velocity Ex	1716.1	1597.9	1468.7	1636.3	1523.8	1401.2
Isp	53.34	49.66	45.65	50.86	47.36	43.55
$\overline{\gamma}$	1.066	1.070	1.076	1.066	1.069	1.076
Ae/At	11.94	11.83	11.65	8.36	8.30	8.19
$\overline{M}$	146.066	→		146.066	→	

Cost: $2.75/lb

APPENDIX B (con't)

GAS - N_2

Boiling Point - 320°F.

P_{ch}, PSIA	1000 →			650 →			1000 →			1500 →		
T_{ch}, F	700	550	400	700	550	400	80 →			115 →		
Pex, PSIA	14.7 →			14.7 →			6.667	5.714	5.000	8.571	7.500	6.667
Tex, F	-94.4	-148	-198	-48.7	-108	-164						
P_c/P_e	68.05 →			44.2 →			150	175	200	175	200	225
Cp Ex	6.985	7.004	7.027	6.974	6.990	7.011						
γ Ex	1.398	1.396	1.394	1.398	1.397	1.395						
Density	.0017	.0020	.0024	.0015	.0018	.0021						
Viscosity	142	125	108	153	138	122						
Velocity	3209.	2983.	2744.	3116.	2897	2666						
Mach No.	3.37	3.39	3.41	3.09	3.10	3.12	4.01	4.12	4.23	4.12	4.23	4.32
Isp	99.75	92.72	85.29	96.84	90.04	82.85						
$\bar{\gamma}$	1.387	1.391	1.393	1.388	1.391	1.394	1.394	1.393	1.393	1.394	1.393	1.393
$\rho v/\mu$	.0384	.0477	.0609	.0305	.0378	.0459	.0864	.0815	.0755	.1129	.1039	.0983
$\bar{M}$	28.016			28.016			28.016			28.016		

Cost: $0.36/lb.

APPENDIX B (Con't)

GAS - Ar

BOILING POINT - 187.6°F

P_{ch}, psia	1000 →			650 →		
T_{ch}, psia	700	550	400	700	550	400
P_{ex}, psia	14.696 →			14.696 →		
T_{ex}, F	-245.13	-272.88	-300.63	-204.80	-237.77	-270.74
C_p CH	4.970	4.970	4.970	4.970	4.970	4.970
γ CH	1.666	1.666	1.666	1.666	1.666	1.666
Density Ch	.0509	.0587	.0694	.0332	.0383	.0452
Viscosity	403	370	340			
Cp Ex	4.970	4.970	4.970	4.970	4.970	4.970
γ Ex	1.666	1.666	1.666	1.666	1.666	1.666
Density Ex	.0041	.0048	.0056	.0035	.0040	.0047
Viscosity Ex	112	100	88	130	116	101
Velocity Ex	2425.7	2263.4	2088.5	2373.4	2214.6	2043.5
I_{sp}	75.39	70.35	64.91	73.77	68.83	63.51
$\overline{\gamma}$	1.666	1.666	1.666	1.666	1.666	1.666
A_e/A_t	4.53	4.53	4.53	3.57	3.57	3.57
$\overline{M}$	39.948 →			39.948 →		

Cost: $0.13/lb

APPENDIX B (Con't)

GAS - CO_2

BOILING POINT - 109.3°F

P_{ch}, psia	1000	→		650	→	
T_{ch}, F	700	550	400	700	550	400
Pex, psia	14.696	→		14.696	→	
Tex, F	101.74	13.14	-73.88	144.89	51.21	-41.00
C_p, CH	11.560	11.054	10.467	11.560	11.054	10.467
γ CH	1.208	1.219	1.234	1.208	1.219	1.234
Density Ch	.0777	.0905	.1085	.0495	.0576	.0687
Viscosity Ch	290	258	245			
Cp Ex	9.029	8.525	7.993	9.261	8.746	8.198
γ Ex	1.282	1.304	1.331	1.273	1.294	1.320
Density Ex	.0017	.0021	.0025	.0016	.0019	.0023
Viscosity Ex	163	141	126	173	150	126
Velocity Ex	2804.2	2597.6	2374.7	2701.2	2503.8	2290.9
Mach No.	3.12	3.12	3.12	2.90	2.90	2.90
Isp	87.16	80.73	73.81	83.96	77.82	71.20
$\overline{\gamma}$	1.245	1.262	1.283	1.240	1.257	1.277
A_e/A_t	8.14	7.90	7.61	6.01	5.86	5.67
$\overline{M}$	44.011	→		44.011	→	

Cost: $0.17/lb

APPENDIX B (Con't)

GAS - N_2O

BOILING POINT - 129.1°F

P_{ch}, psia	1000	→		650	→	
T_{ch}, F	700	550	400	700	550	400
Pex, psia	14.696	→		14.696	→	
T_{ex}, F	110.80	21.13	-66.03	153.64	58.96	-33.36
C_p CH	11.821	550	10.736	11.821	11.304	10.736
γ CH	1.202	1.213	1.227	1.202	1.213	1.227
Density Ch	.0585	.0684	.0828	.0376	.0438	.0525
Viscosity Ch	290	261	237			
Cp Ex	9.503	9.083	8.658	9.697	9.262	8.819
γ Ex	1.264	1.280	1.298	1.258	1.273	1.291
Density Ex	.0017	.0020	.0025	.0016	.0019	.0023
Viscosity	165	142	117	176	152	125
Velocity Ex	2814.0	2607.0	2385.1	2709.8	2512.1	2299.9
Mach No.	3.12	3.13	3.13			
Isp	87.46	81.03	74.13	84.22	78.08	71.48
$\overline{\gamma}$	1.233	1.247	1.262	1.230	1.243	1.259
A_e/A_t	8.32	8.11	7.88	6.12	5.98	5.83
$\overline{M}$	44.014	→		44.014	→	

Cost: $0.60/lb

APPENDIX C

EQUATIONS DESCRIBING OPERATION OF THE APPARATUS
(See Nomenclature for Most Symbols)

1. System Schematic

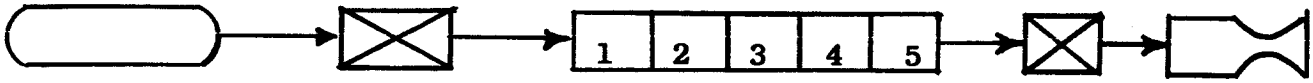

2. Tank

a. Temp. Constant at 212°F
b. Volume Constant at 5 ft^3
c. Pressure:

$$P_{tk} = P_{tk} - \left(\frac{RT_{tk}}{\overline{M} V_{tk}}\right) \int \dot{w} V \, dt \qquad (1)$$

3. Regulator

Isentropic expansion:

$$T_o = T_{tk} \left[\frac{P_k}{P_{tk}}\right]^{\left(\frac{\gamma-1}{\gamma}\right)} \qquad (2)$$

(T_o is the gas temperature entering the first node of the heater.)

4. Heater

For each node we have the following system of equations:

a. $$\dot{Q}_{gas} = C_p \cdot \dot{W}_v \, (T_n - T_{n-1}) = \left[T_{nm} - \left(\frac{T_n + T_{n-1}}{2}\right)\right] .H \qquad (3)$$

T_n is the output temperature of the n^{th} node, T_{n-1} is the gas input temperature and T_{nm} is the metal temperature in that node.

b. $$T_{nm} = T_{nm_o} + \frac{1}{(C_p \dot{W})_m} \int (\dot{Q}_{in} - \dot{Q}_{gas}) \, .dt \qquad (4)$$

($\dot{Q}_{in}$ is the steady heat input from the electrical heaters)

c. $$T_h = \left(\frac{T_{nm}\, H + (C_p\, W_v - .5H)\, T_{n-1}}{C_p\, \dot{W}_v + .5H} \right) \quad (5)$$

5. Valve

a. $$A_v = \int_0^{t_x} \dot{A}_v \, dt \quad (6)$$

where A_v = valve area and t_x represents total opening time.

b. $$\dot{W}_v = \frac{5.21 \cdot A_v \cdot P_r}{\sqrt{R\, T_5}} \left[.F \left(\frac{P_c}{P_r} \right) \right] \quad (7)$$

where $$F\left(\frac{P_c}{P_r}\right) = \sqrt{\frac{\gamma}{\gamma-1}\left[\left(\frac{P_c}{P_r}\right)^{2/\gamma} - \left(\frac{P_c}{P_r}\right)^{\gamma-1/\gamma}\right]}$$

Except when $P_c/P_r = \left(\frac{2}{\gamma-1}\right)^{\gamma/\gamma-1}$ = (critical pressure). Then use

$\left(\frac{2}{\gamma-1}\right)^{\frac{\gamma}{\gamma-1}}$ instead of (P_c/P_r) in $F\ \frac{P_c}{P_r}$

6. Chamber

a. $$\dot{W}_{in} = \dot{W}_v \quad (8)$$

b. $$\dot{W}_{out} = \frac{7.78\, A_n P_c}{\sqrt{R\, T_c}}\, F\left(\frac{P_a}{P_c}\right) \quad (9)$$

where $F\left(\frac{P_a}{P_c}\right)$ is defined in a manner similar to $F\left(\frac{P_c}{P_k}\right)$

c. $$W_c = \int (\dot{w}_{out} - \dot{w}_{in})\, dt \quad (10)$$

d $$T_{in} = T_5 \left(\frac{P_c}{P_r}\right)^{\gamma-1/\gamma} \quad (11)$$

e. $$T_c = T_{c_o} + \int \frac{\left(\dot{W}_v T_{in} - \dot{W}_{out} T_c\right) \cdot dt}{W_c} \qquad (12)$$

(assumes mixing of inlet gas with chamber gas)

f. $$P_c = \frac{W_c . R . T_c}{M \cdot V_c} \qquad (13)$$

These equations were programmed on an analog computer. The block diagram of the computer circuitry is shown on the next page (Figure 18).

APPENDIX D

Example of Data Reduction Method

The data of run No. 2AX4025 has been reproduced in Figure 19 to provide an example of how it was reduced. If there is no pressure on the system, the positions of the galvonometer traces are the "zero" points. These correspond to ambient temperature and pressure. The "R-cals", provided at the beginning and end of each day of testing indicate the level of the traces when a known pressure signal is applied. The difference between the galvonometer deflection at "zero" and "R cal" is the "net R cal". Similarly the difference between the deflections during a run and at zero is called "net reading". Deflections are measured from a datum trace at the edge of the paper.

The data is reduced as follows:

(1) Net R cal is measured in inches. In this case for Pch (trace 25) it is 0.470 in.

(2) K value equals known pressure signal/net R cal. In this case it is 105.3 psi/inch.

(3) Net reading is determined. In this case 9.340 in.

(4) Net reading multiplied by K to determine Pch which is psig.

(5) Add barometric pressure reading (taken twice each day) giving Pch=997.80 psia.

(6) Repeat all above steps for other pressures.

(7) The highest chamber pressure (stagnation) is divided by each nozzle pressure in turn. In this case, the pressure ratios are P_c/P_e=23.71 at an area ratio of 4.06 and P_c/P_e=75.9 at an area ratio of 9.1.

(8) The temperature R cal represents 150 degrees F. The zero represents ambient temperature. Knowing the ambient temperature and the 150 degrees F trace deflection enables a relation to be found between Tc and deflection.

(9) Ae/At are used as inputs to the Simulant Characterization Program (discussed in Appendix A) which computes the theoretical Pc/Pe and $\overline{\gamma}$.

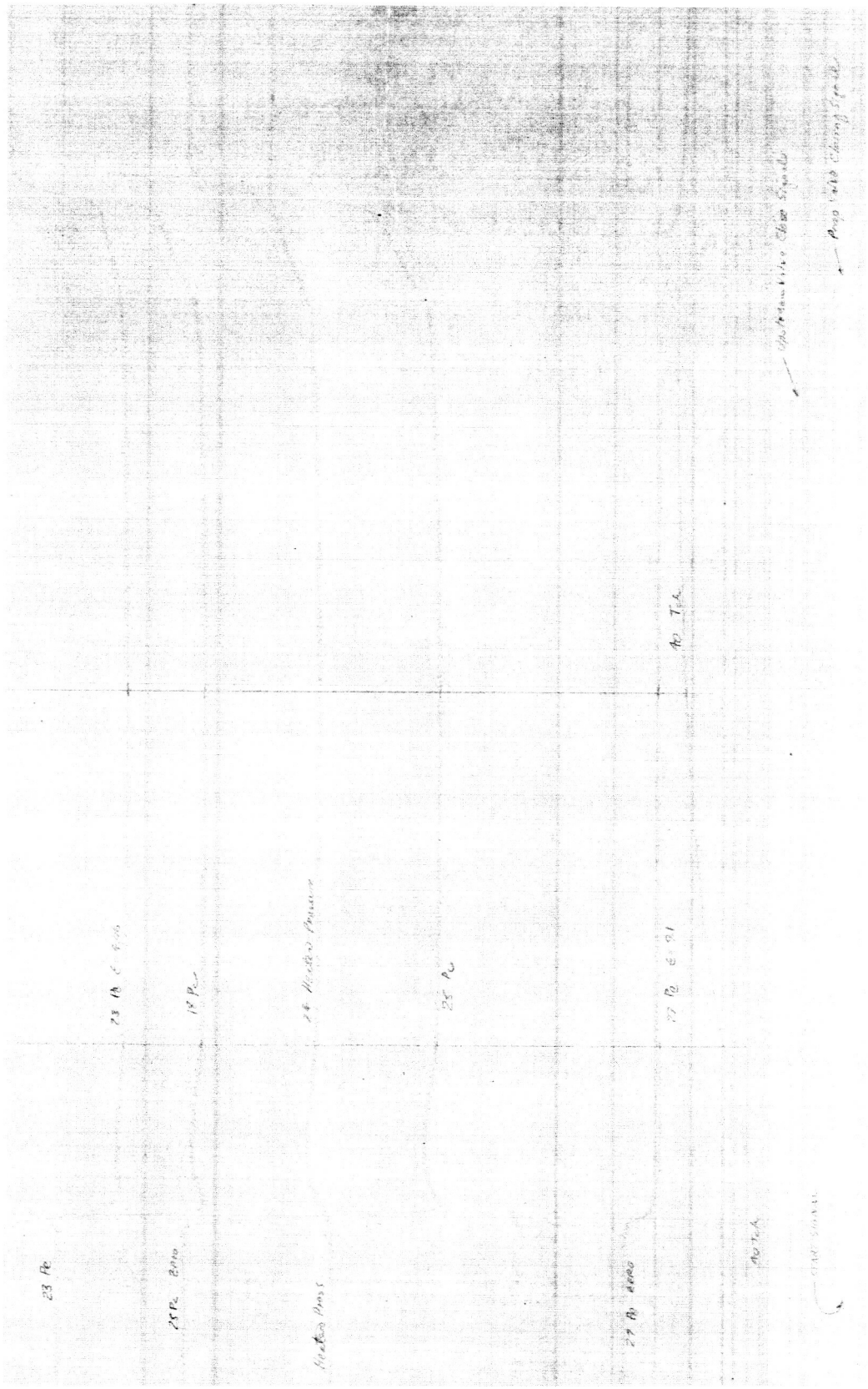

Figure 19. Sample of Data

(10) Experimental $\overline{\gamma}$ is computed from the relation

$$\frac{A_e}{A_t}\left(\frac{P_c}{P_0}\right)^{\frac{\gamma-1}{\gamma}}\left(1+\frac{\gamma-1}{2}\right)^{\gamma+3/2(\gamma-1)} = \left[1+\frac{\gamma-1}{2}+\frac{\gamma-1}{2}\left(\frac{P_e}{P_c}\right)^{\frac{\gamma-1}{\gamma}}\right]^{\gamma+1/2(\gamma-1)}$$

which was plotted for the two area ratios to simplify and speed data reduction. In the case described, the theoretical $\overline{\gamma}$ was 1.238 at A_e/A_t = 4.06 and 1.245 at A_e/A_t = 9.1. The experimental was 1.253 at 4.06 and 1.267 at 9.1. The value of γ at any point may be computed by plotting $\overline{\gamma}$ vs. A_e/A_t. The γ values are then approximately equal to the $\overline{\gamma}$ values at twice the A_e/A_t of interest. In general the values of γ and $\overline{\gamma}$ follow the same trends and remain close together.